BIOMARKERS: REVIEW AND APPLICATION TO

THE EAGLE FORD SHALE

FORMATION

by

UGOCHUKWU ONONOGBU

Presented to the Faculty of the Graduate School of

The University of Texas at Arlington in Partial Fulfillment

of the Requirements

for the Degree of

MASTER OF SCIENCE IN GEOLOGY

THE UNIVERSITY OF TEXAS AT ARLINGTON

December, 2012

ACKNOWLEDGEMENTS

ABSTRACT

BIOMARKERS: REVIEW AND APPLICATION TO

THE EAGLE FORD SHALE

FORMATION

Ugochukwu Ononogbu, M.S.

The University of Texas at Arlington, 2012

Supervising Professor: Qinhong Hu

Biomarkers have become an integral part of oil exploration. Gas Chromatography (-Mass Spectrometry) is performed to an oil sample to acquire biomarkers from the sample. The presence, lack of, or abundance of a given compound (or biomarker) in the geochemical results of an oil sample depict(s) a property or properties of the source rock and the oil. For example, the abundance of pristane and lack of phytane in an oil sample are characteristic of a shale source rock, such as the Eagle Ford, will show a high pristane to phytane ratio.

The Eagle Ford shale formation is cretaceous in age; the presence and absence of certain biomarkers like oleanane suggest age ranges. The oil sample tested from the Eagle Ford shale formation support a source rock from the Cretaceous period. The biomaker results from the Eagle Ford shale formation also suggest the thermal maturity of oil samples tested. The Eagle Ford shale formation produces both gas and oil. Formations which produce both oil and gas ensure that the biomarkers detected can be used to study thermal maturity. The results from the Eagle Ford shale formation show a thermal maturity that is between peak and late stages of oil generation which supports continued exploration from the reservoir of the oil sample.

Results are affected by many variables; therefore, there will be considerable variations in the ensuing interpretations. The use of multiple biomarkers in the results from the Eagle Ford shale formation and comparing and contrasting those results with other available results will produce more accurate conclusions.

TABLE OF CONTENTS

LIST OF ILLUSTRATIONS

LIST OF TABLES

CHAPTER 1

INTRODUCTION

1.1 Introduction to Biomarkers

Biomarkers are compounds found in oil that hold information of the oil. They are mainly lipids from living organisms that have been preserved through time. Unlike other organic molecules such as proteins and carbohydrates, lipids can be preserved in sediments for millions of years in a stable condition. A stable condition has very little to no free-oxygen (anoxic condition) and minimal erosion.

Biomarkers are primarily made up of carbon and hydrogen, but can also contain other elements such as oxygen, nitrogen, sulfur, and iron. Biomarkers are generally used in age dating of a locale in the search for evidence of life and in petroleum exploration. In petroleum exploration, biomarkers are indicative of one or more of the following: geologic time, thermal maturity, and/or depositional environment. An example of a geologic time biomarker would be oleanane (18alpha-oleanane) in an oil sample which indicates that the oil is from Cretaceous; oleanane is formed from a flowering plant called angiosperm which is unique to Cretaceous and younger (Moldowan et al., 1994). Furthermore, as an example of a depositional environment: pristane/phytane ratio of less than one (< 1) in oil indicates that the environment was hypersaline. Environments with increasing paleosalinity show a decreasing ratio of pristane/phytane (ten Haven et al., 1987). The Eagle Ford shale formation is a marine environment and not hypersaline; therefore, the ratio of pristane/phytane would be greater than 1. Table 1.1 shows more examples of biomarkers that provide information about the age of the source rock, the depositional environment and the thermal maturity.

Table 1.1 Biomarkers indicative of source rock age, depositional environment and thermal maturity

Biomarker(s)	Indication	Comments
Oleanane	Indicative of a source rock from the Cretaceous Period	Indicative of Cretaceous and younger (Moldowan et al., 1994)
Pristane/Phytane	Indicative of marine (oxic) or carbonate (suboxic) depositional environment.	Ratio greater than 1 indicates marine (Didyk et al., 1978)
Saturate compounds - Steranes: S/(S+R)	Tells the thermal maturity of oil samples, but could increase dramatically past the oil peak generation.	A high ratio indicates high thermal maturation and/or heavy biodegrading (Seifert and Moldowan, 1986)
Aromatic Compounds- Triaromatic/(Monoaromatic + Triaromatic)	Tells the thermal maturity of samples through the oil window. The value increases with maturity.	The ratio works because Triaromatic is a more mature Monaromatic. Applications of the ratio have been applied to basin models (Mackenzie, 1984)

Biomarkers are evaluated from analysis on an oil sample using Gas Chromatography or Gas Chromatography-Mass Spectrometry (GC-MS). Weatherford Laboratories and Oil Tracers used a GC-MS instrument to test an oil sample from the Eagle Ford shale formation. Several of the resulting compounds in the oil were known biomarkers; therefore, the oil sample was further subjected to the GC-MS tests. A majority of the compounds (biomarkers) derived from the GC-MS tests are indicators of the age of the source rock, the source rock depositional environment, and thermal maturity.

<div align="center">1.2 Physical Geology of Eagle Ford Formation</div>

The formation is located from the Mexican border northeastward into East Texas. The formation lies between the Austin Chalk and the Buda lime (Fig. 1) around 4,000 to 12,000 feet below the earth surface, with a thickness around 250 feet. The formation is about 50 miles wide and 400 miles long (Fig. 2) and believed to be Cretaceous in age. The Eagle Ford formation is divided into two layers: shale at the bottom which is organically enriched (Liro et al., 1994), and carbonate flagstone interbedded with shale above. The Eagle Ford shale formation is the likely source of the 140,000 acre East Texas oil field (Liro et al., 1994), which provides hydrocarbons for formations like the Austin Chalk (Railroad Commission of Texas, 2012).
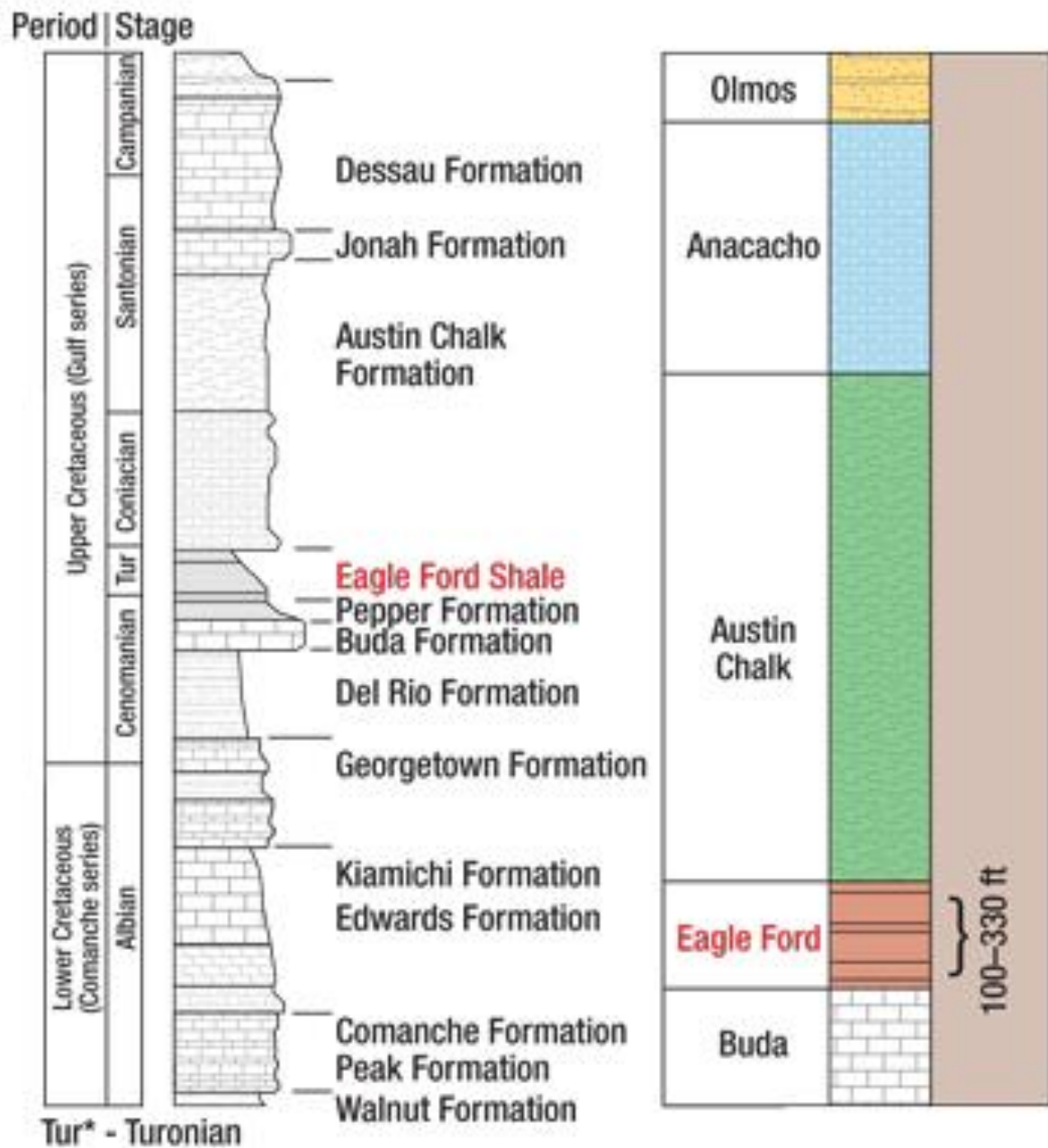
Figure 1.1 Eagle Ford shale formation lying between the Buda and Austin Chalk formation (World Oil, 2012)
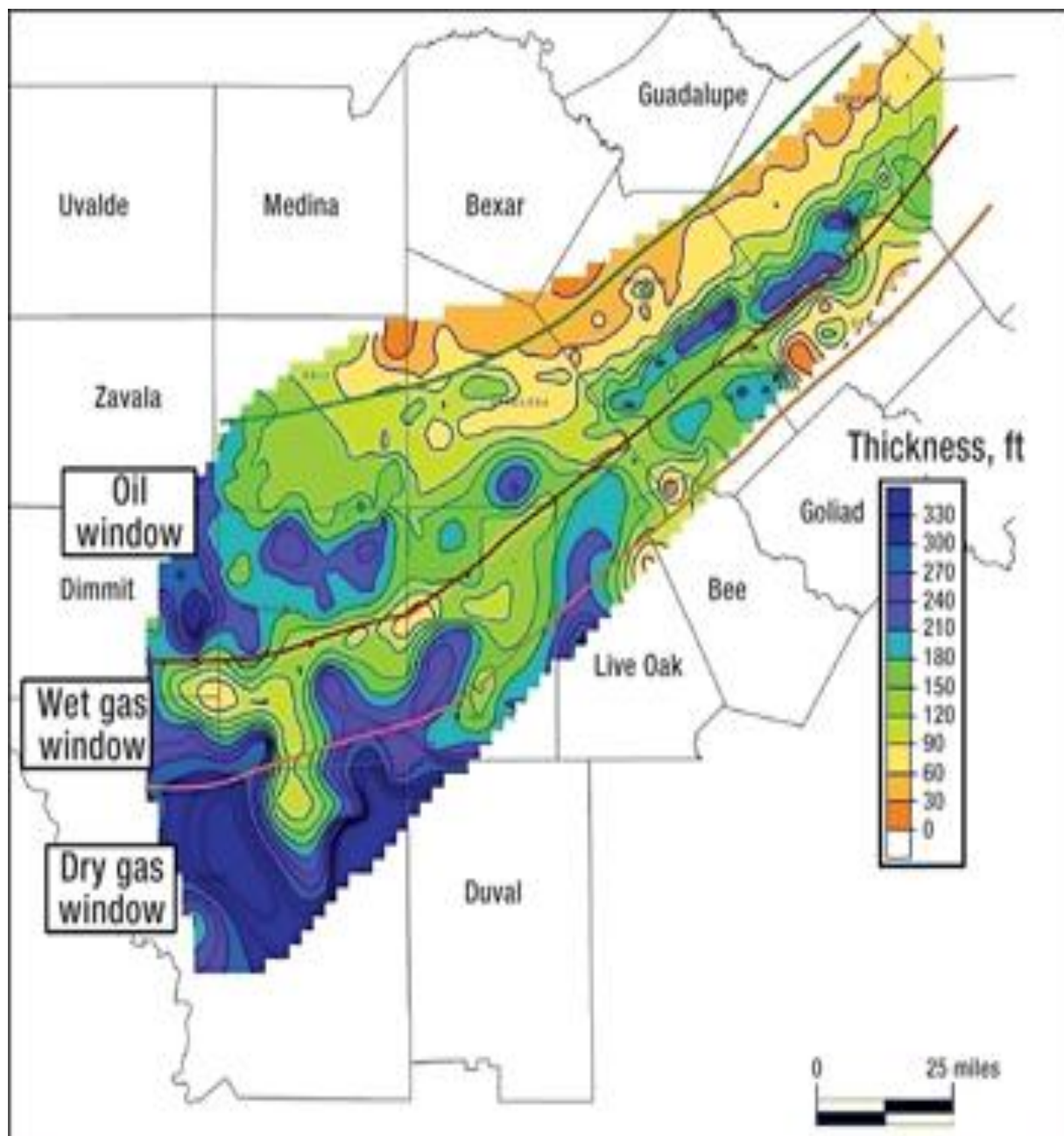
Figure 1.2 Eagle Ford shale formation through Texas showing changes in thickness (World Oil, 2012)

CHAPTER 2

PREVIOUS RESEARCH OF BIOMARKERS

There is a significant amount of information on biomarkers in the petroleum exploration field; detailed papers discussing biomarkers started to be published in the 1970s. Petroleum exploration companies like Exxon Mobil have supported the study of biomarkers over the years making biomarkers an important aspect of petroleum exploration. Scientists, including Kenneth E. Peters, Clifford C. Walters, and J. Michael Moldowan have published many papers and books on biomarkers including volumes 1 and 2 of The Biomaker Guide; their findings from Volume 2 of the book is incorporated into this research. GeoMark Research, Inc owns a library called Oil Information Library System (http://www.geomarkresearch.com/). The library contains a lot of information on biomarkers, including various GC and GC-MS results of oils throughout the geologic time. Weatherford Laboratories and Oil Tracers have also researched biomarkers for many years, and they donated the analytical results for an oil sample from the Eagle Ford shale formation for this research.

CHAPTER 3

AIM AND OBJECTIVE OF THIS RESEARCH

The objective of this study is to further understand the use of biomarkers in petroleum exploration. To accomplish the objective, I used literature papers and biomarker books as a guide while synthesizing the oil sample biomarker analyses from the Eagle Ford shale formation. The overall aim of this study is to use the biomarkers found in the oil sample to determine: 1) the age of the source rock, 2) the depositional environment, and 3) the thermal maturity of the oil in the Eagle Ford shale formation. Other information like the kind of organic matter(s) that went through diagenesis to form biomarker(s) found in the oil will also be explored during the research.

CHAPTER 4

METHOD

4.1 Sample Collection

Weatherford Laboratories and Oil Tracers collect oil samples at the well head without contamination. The oil sample used in this study was collected in the Eagle Ford shale in an undisclosed location because of proprietary reasons. The well head is the structural support of a well located at the surface of the well. A component called the header connects well head(s) to flowlines, it has producing and testing valves that control the flow of each well. The sample was not taken from the header because it could be contaminated by leaking valves, corrosion, etc. Although it may be easier to collect the oil sample from components like the header, potential contamination being in the tested sample is not an acceptable practice at Weatherford Laboratories and Oil Tracers. In addition, the sample was collected in a glass bottle. Other sample storage containers like plastic bottles may contaminate the sample.

4.2 Gas Chromatography (GC)

GC is the process of separating and identifying different organic compounds within a test sample. Figure 4.1 below shows the brief process; the test sample is injected into the GC instrument where the carrier gas (usually helium) takes it through the various components of the GC instrument. The first GC instrument component is the column (a thin tube) with its interior lined with a polymer coating (usually silicone oil polymers and other organic chemicals). The polymer reacts with each compound in the sample differently as the carrier gas takes the sample through the column, which is in the oven. The oven heats up the column turning the compounds in the sample into a gaseous state; therefore, the more volatile material will get to the next component faster with a smaller retention time. The next component the gaseous material encounters is the detector which records the concentration (peak area or peak height)

of eluted compound over time Finally, the test sample can be fully recovered if the exit port is connected to a cooling component, by changing the gaseous material back into liquid form (expelling the helium).
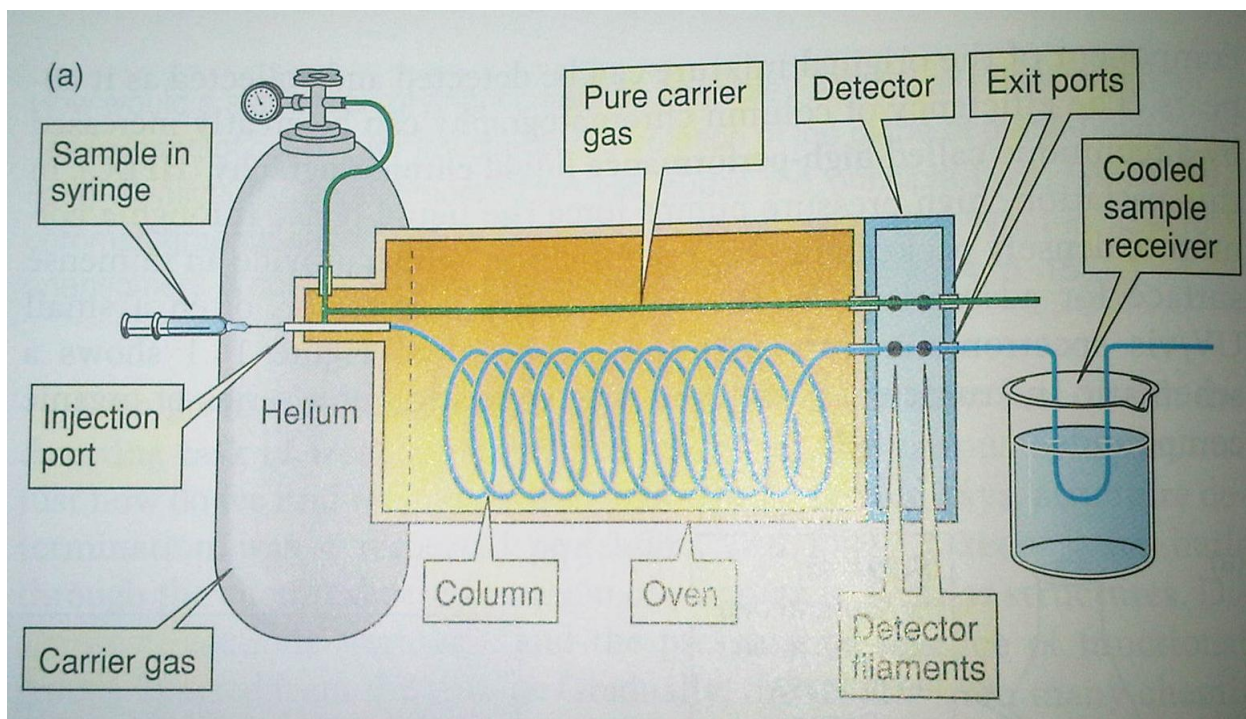
Figure 4.1 A schematic view of a Gas Chromatograph (Maitland, 2000)

4.3 Gas Chromatography - Mass Spectrometry (GC-MS)

After the GC analysis was done on the oil sample, the results were analyzed and the ratios and compounds acquired can be seen on Figure 5.2 and Table 5.1. The GC results showed the presence of saturated and aromatic biomarkers, GC-MS analysis was conducted to measure the saturated fraction and the aromatic fraction of the oil sample separately. The GC-MS has a two part process, the GC and MS. The MS instrument is connected to the GC instrument's exit port, beginning the MS process immediately when the sample is injected in GC. A cathode in MS reacts with the incoming material making it positively charged. Figure 4.2 illustrates the MS process, the positively charged material (ions) flows towards the negatively

charged plate. The slit on the plate allows some of the ions through to a curved path which is between the poles of a magnet. The strength of the magnet is set to allow a certain molecular weight to pass through the curve path successfully, hence filtering unwanted results. Figure 5.3 and 5.4 show multiple molecular weight (m/z) values, each value represents the molecular weight allowed through the curved path. The ion detector then produces a graph/trace of ionic abundance versus time. The aromatic GC-MS was run with ortho-terphenyl (seen in Table 5.4), and the saturated GC-MS was run with 5 beta-cholane (seen in Table 5.2). Both compounds (ortho-terphenyl and 5 beta-cholane) are internal standards used to calibrate the concentration of each compound in the oil sample as a ratio of the internal standard to measured compound.
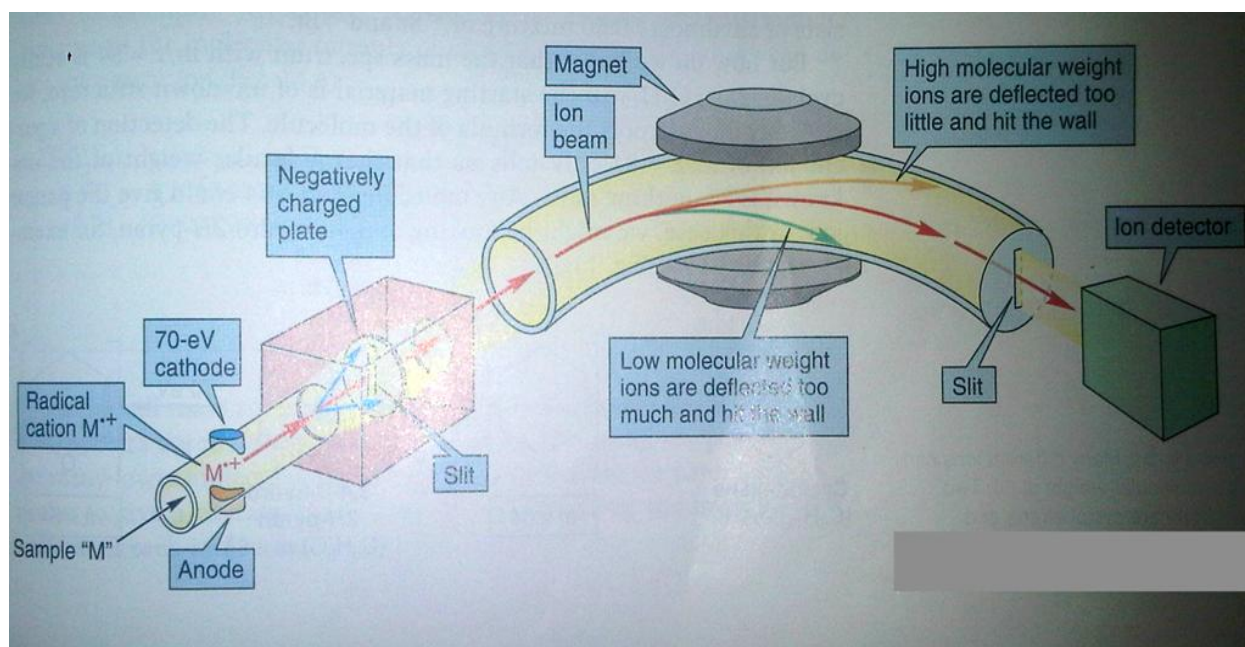
Figure 4.2 A schematic view of a Mass Spectrometer (Maitland, 2000)

CHAPTER 5

RESULTS

5.1 Example Results of GC and GC-MS Analyses

Figure 5.1 (from <u>The Biomarker Guide</u>) shows a whole oil GC and a saturate GC-MS results of an oil sample from the Eagle Ford shale formation. The values of Pr/n-C17 and Ph/n-C18 are used to evaluate the thermal maturity of oil (Winters and Williams, 1969). Another example is the pristane/phytane value; it is greater than one in shales. I'll compare the results in Figure 5 to results of oil from my Eagle Ford oil sample as well as from other source rocks, to further explain the usage of biomarkers.

GEOCHEMICAL SUMMARY SHEET

Country: **USA**   Depth: **3600'**   02-Jul-99
Basin: **Onshore GOM**   Age: **U. Cretaceous**   Sample ID: **TX129**
Field: **East Texas**   Formation: **Woodbine**   LAT: 32.24
Well: **Langston #T-1**   LONG: -94.95

BULK PROPERTIES   API Gravity: **38.0**   % S: **0.27**   ppm V: **1.9**
    %< C15: **41.9**   ppm Ni: **3.0**

C15 + Composition
   % Sat: **56.0**
   % Aro: **26.9**
   % NSO: **15.8**
   % Asph: **1.3**
   Sat/Aro= **2.08**
   n-Paraffin/Naphthene= **0.19**

Relative % — %Asph, %NSO, %Aro, %Sat (0, 20, 40, 60)
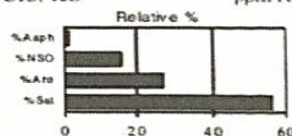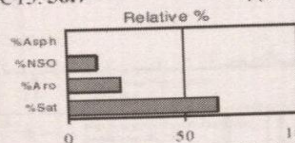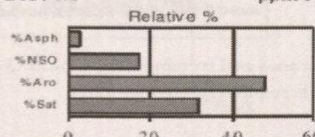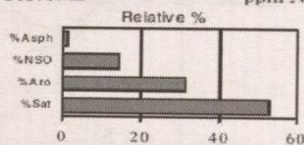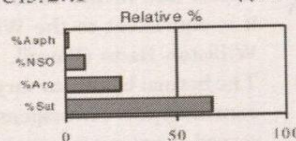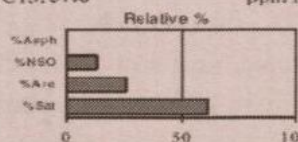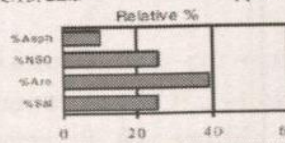
Stable Carbon Isotope Composition
δ per mil PDB
C15+ Saturate: **-28.75**
C15+ Aromatic: **-27.07**
Canonical Variable: **0.99**

Miscellaneous:

FID1 A, (GOM\TX129.D)

WHOLE CRUDE GAS CHROMATOGRAPHY
Pr/Ph= **1.80**
Pr/n-C17= **0.71**
Ph/n-C18= **0.47**
n-C27/n-C17= **0.32**
CPI= **1.061**

BIOMARKERS   ppm C30 Hopane: **473**

Ion 191.00: 2901042.D — Terpanes

Ion 217.00: 2901042.D — Steranes

OilMod Ratios
C19/C23= **0.12**
C22/C21= **0.46**
C24/C23= **0.74**
C26/C25= **1.08**
Tet/C23= **0.41**
C27T/C27= **0.02**
C28/H= **0.02**
C29/H= **0.36**
C30X/H= **0.14**
OL/H= **0.02**
C31R/H= **0.27**
GA/C31R= **0.27**
C35S/C34S= **0.72**
Ster/Terp= **0.58**
Rearr/Reg= **2.45**
%C27= **31.2**
%C28= **36.4**
%C29= **32.4**
C29 20S/R= **0.78**
Ts/Tm= **1.93**
C29D/H= **0.63**
DM/H= **0.01**

COMMENTS: Upper Cretaceous Eagle Ford Shale

Figure 5.1 Eagle Ford shale formation showing whole oil GC and saturate compound GC-MS traces with important values/ratios (Peters et al., 2005)

5.2 Acquired Results

The first set of results are the whole oil GC results; the trace/graph (Figure 5.2, key biomarkers are highlighted) which is followed by a table showing all the compounds recorded by the detector in the GC instrument (Table 5.1). The trace shows various peaks with peak labels. The peak labels can be matched to the table which gives some information of each peak. The ratios under the trace are ratios of biomarkers that suggest certain properties of oil.

The next set of results is the saturate GC-MS; the trace, followed by a table of the detected compounds, and later a table showing the important ratios which can be seen to the right of the trace (Figure 5.3, key biomarkers are highlighted). Three traces are of three different ions as "m/z" numbers (Section 4.3). The ratios to the right of the traces are ratios of the biomarkers from the Table 5.2. The applications of the ratios are specified to the right of ratio values: A stands for age of rock; D stands for depositional environment; and M stands for maturity. The ratios can also be seen in greater detail in Table 5.3.

The final set of results is the aromatic GC-MS (Figure 5.4, Table 5.4, and Table 5.5) which has the same layout as the saturate GC-MS.

Weatherford LABORATORIES

WHOLE OIL GC

Company:		Client ID:	
Country:		Project #:	
Basin:		Lab ID:	
Lease:		Sample Type:	OIL
Block:		Sampling Point:	
Field:		Formation:	Eagle Ford
Well Name:		Geologic Age:	
Latitude:		Top Depth:	
Longitude:		Bottom Depth:	

Whole Oil GC Trace   G3080120.D

WGC parameters	
Pristane/Phytane	1.53
Pristane/nC_{17}	0.65
Phytane/nC_{18}	0.51
nC_{18}/nC_{19}	1.09
nC_{17}/nC_{20}	1.45
CPI Marzi	1.04
Normal Paraffins	34.7
Isoprenoids	5.1
Cycloparaffins	8.3
Branched (iso-) Paraffins	5.2
BTX aromatics	1.9
Resolved unknowns	44.7

Thompson[1]		
A.	BZ/nC_6	0.09
B.	TOL/nC_7	0.46
C.	$(nC_6+nC_7)/(CH+MCH)$	1.12
I.	Isoheptane Value	0.62
F.	nC_7/MCH	0.74
U.	CH/MCP	0.57
R.	$nC_7/2MH$	3.14
S.	$nC_9/22DMB$	130.09
H.	Heptane Value	19.46
	MCH/nC_7	1.34
	$mpXYL/nC_8$	0.37

Mango[2]	
P_1	18.95
P_2	14.32
P_3	4.61
$5N_1$	11.81
N_2	16.05
$6N_1$	34.26
K_1	0.94
K_2	0.47
$5N_1/6N_1$	0.34
P_2/N_2	0.29
$\ln(24DMP/23DMP)$	-1.07

Halpern[3]	
Tr_1	2.58
Tr_2	5.55
Tr_3	2.43
Tr_4	1.77
Tr_5	4.19
Tr_7	1.79
Tr_8	3.13
C_1	0.04
C_2	0.58
C_3	0.20
C_4	0.04
C_5	0.14

[1]Thompson, K.F.M.,1983.GCA V.47, p.303. [2]Mango, F.D.,1994.GCA: V.58, p.895. [3]Halpern,H.I.,1995,AAPG Bull. V.79, p.801. [4]Marzi,1993,OrgG,20,1301.

Figure 5.2 Whole Oil GC Trace

Table 5.1 Compounds detected in the whole oil

Company:	Client ID:
Well Name:	Project #:
Depth: -	Lab ID:
Sampling Point:	File Name:

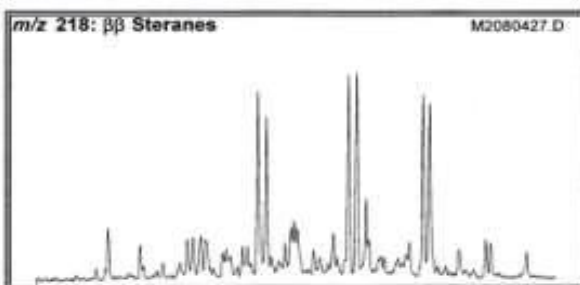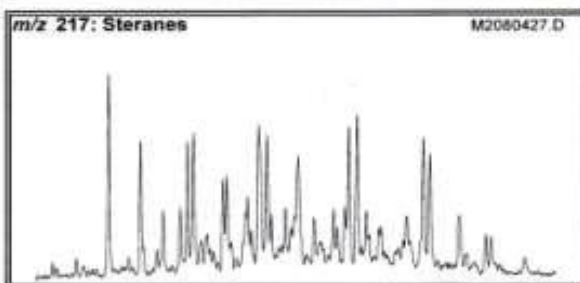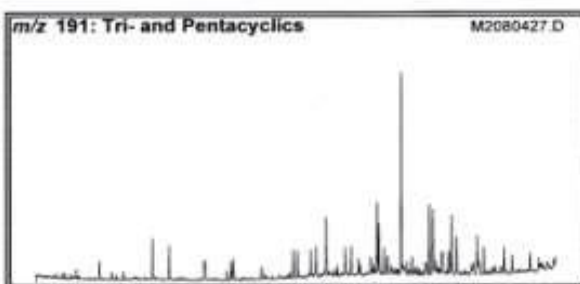| Peak Label	Compound Name	Ret. Time	Area	Height	ppt (Area)	ppt (Hght)
IC4	Iso-alkane C4	4.115	16447	14010	1.61	3.06
NC4	Normal Alkane C4	4.229	99241	82605	9.68	18.06
IC5	Iso-alkane C5	4.653	72394	56233	7.06	12.29
NC5	Normal Alkane C5	4.887	110503	82440	10.78	18.02
22DMB	2,2-Dimethylbutane	5.328	695	466	0.07	0.10
CP	Cyclopentane	5.781	20919	12577	2.04	2.75
23DMB	2,3-Dimethylbutane	5.810	3839	3293	0.38	0.72
2MP	2-Methylpentane	5.892	57175	36667	5.58	8.02
3MP	3-Methylpentane	6.182	36253	22101	3.54	4.83
NC6	Normal Alkane C6	6.582	90414	53695	8.82	11.74
22DMP	2,2-Dimethylpentane	7.239	914	574	0.09	0.13
MCP	Methylcyclopentane	7.295	75086	40275	7.33	8.80
24DMP	2,4-Dimethylpentane	7.428	4037	2076	0.39	0.45
223TMB	2,2,3-Trimethylbutane	7.581	198	74	0.02	0.02
BZ	Benzene	8.050	7993	3581	0.78	0.78
33DMP	3,3-Dimethylpentane	8.246	799	367	0.08	0.08
CH	Cyclohexane	8.357	42697	20622	4.17	4.51
2MH	2-Methylhexane	8.736	26924	13198	2.63	2.89
23DMP	2,3-Dimethylpentane	8.785	11784	5758	1.15	1.26
11DMCP	1,1-Dimethylcyclopentane	8.872	15223	7074	1.49	1.55
3MH	3-Methylhexane	9.071	36931	17579	3.60	3.84
1C3DMCP	1-cis-3-Dimethylcyclopentane	9.300	29073	13553	2.84	2.96
1T3DMCP	1-trans-3-Dimethylcyclopentane	9.413	27314	12636	2.67	2.76
3EP	3-Ethylpentane	9.474	2850	2283	0.28	0.50
1T2DMCP	1-trans-2-Dimethylcyclopentane	9.525	46114	20876	4.50	4.56
NC7	Normal Alkane C7	10.114	84516	38536	8.25	8.42
ISTD	Internal Standard	10.332	35568	15875	3.47	3.47
MCH	Methylcyclohexane	10.953	113619	45763	11.09	10.00
113TMCP	1,1,3,-Trimethylcyclopentane	11.117	20861	8784	2.04	1.92
ECP	Ethylcyclopentane	11.525	6549	2738	0.64	0.60
124TMCP	1,2,4-Trimethylcyclopentane	11.967	16119	6673	1.57	1.46
123TMCP	1,2,3-Trimethylcyclopentane	12.333	18386	7492	1.79	1.64
TOL	Toluene	12.654	39218	15080	3.83	3.30
NC8	Normal Alkane C8	15.289	86964	30078	8.48	6.58
IP9	Isoprenoid C9	17.149	30452	11257	2.97	2.46
MXYL	m-Xylene	18.359	25614	9419	2.50	2.06
PXYL	p-Xylene	18.427	6295	2366	0.61	0.52
OXYL	o-Xylene	19.615	19149	5967	1.87	1.30
NC9	Normal Alkane C9	21.018	73437	25537	7.17	5.58
IP10	Isoprenoid C10	22.994	22520	7594	2.20	1.66
NC10	Normal Alkane C10	26.610	67317	22974	6.57	5.02
IP11	Isoprenoid C11	27.906	22547	7559	2.20	1.65
NC11	Normal Alkane C11	31.871	70245	23163	6.85	5.06
NC12	Normal Alkane C12	36.793	65264	21580	6.37	4.72
IP13	Isoprenoid C13	37.531	23131	6913	2.26	1.51
IP14	Isoprenoid C14	40.293	17277	5548	1.69	1.21
NC13	Normal Alkane C13	41.406	68431	21576	6.68	4.72
IP15	Isoprenoid C15	44.848	23217	7160	2.27	1.57
NC14	Normal Alkane C14	45.741	66924	21179	6.53	4.63
IP16	Isoprenoid C16	48.404	28232	7035	2.75	1.54
NC15	Normal Alkane C15	49.828	72455	20493	7.07	4.48

Table 5.1 Continued

Company:						
Well Name:			Client ID:			
Depth: -			Project #:			
Sampling Point:			Lab ID:			
			File Name:			

Peak Label	Compound Name	Ret. Time	Area	Height	ppt (Area)	ppt (Hght)
NC16	Normal Alkane C16	53.693	62913	19220	6.14	4.20
IP18	Isoprenoid C18	55.624	28872	6001	2.82	1.31
NC17	Normal Alkane C17	57.354	60518	17888	5.90	3.91
IP19	Isoprenoid C19 (Pristane)	57.716	39596	7502	3.86	1.64
PHEN	Phenanthrene	58.740	3290	719	0.32	0.16
NC18	Normal Alkane C18	60.834	50555	15066	4.93	3.29
IP20	Isoprenoid C20 (Phytane)	61.291	25943	4756	2.53	1.04
NC19	Normal Alkane C19	64.147	46314	13314	4.52	2.91
NC20	Normal Alkane C20	67.306	44237	12380	4.32	2.71
NC21	Normal Alkane C21	70.327	39105	11475	3.82	2.51
C25HBI	Highly Branch Isoprenoid C25	70.567	2466	607	0.24	0.13
NC22	Normal Alkane C22	73.217	36638	10681	3.57	2.34
NC23	Normal Alkane C23	75.988	34691	10259	3.38	2.24
NC24	Normal Alkane C24	78.646	32153	9268	3.14	2.03
NC25	Normal Alkane C25	81.202	31264	8769	3.05	1.92
NC26	Normal Alkane C26	83.665	31099	8469	3.03	1.85
NC27	Normal Alkane C27	86.037	32245	8715	3.15	1.91
NC28	Normal Alkane C28	88.328	34739	9515	3.39	2.08
NC29	Normal Alkane C29	90.541	41677	11049	4.07	2.42
NC30	Normal Alkane C30	92.679	42020	11448	4.10	2.50
NC31	Normal Alkane C31	94.747	37208	9732	3.63	2.13
NC32	Normal Alkane C32	96.752	30747	8246	3.00	1.80
NC33	Normal Alkane C33	98.697	28895	7479	2.82	1.64
NC34	Normal Alkane C34	100.581	24246	6065	2.37	1.33
NC35	Normal Alkane C35	102.437	21523	5128	2.10	1.12
NC36	Normal Alkane C36	104.440	16912	3524	1.65	0.77
NC37	Normal Alkane C37	106.684	17072	3046	1.67	0.67
NC38	Normal Alkane C38	109.246	14883	2331	1.45	0.51
NC39	Normal Alkane C39	112.172	10805	1509	1.05	0.33
NC40	Normal Alkane C40	115.588	10328	1172	1.01	0.26
NC41	Normal Alkane C41	119.568	8236	801	0.80	0.18

Weatherford LABORATORIES

SATURATE GCMS

Company:
Country:
Basin:
Lease:
Block:
Field:
Well Name:
Latitude:
Longitude:

Client ID:
Project #:
Lab ID:
Sample Type: OIL
Sampling Point:
Formation: Eagle Ford
Geologic Age:
Top Depth:
Bottom Depth:

m/z 191: Tri- and Pentacyclics   M2080427.D

m/z 217: Steranes   M2080427.D

m/z 218: ββ Steranes   M2080427.D

RATIOS (on Areas)[1]		Appl[2]	TEV[3]
Steranes (m/z 217; 218)			
%C_{27} αββS (218)	28.5	D	
%C_{28} αββS (218)	38.0	D	
%C_{29} αββS (218)	33.5	D	
%C_{27} αααR (217)	28.3	D	
%C_{28} αααR (217)	34.0	D	
%C_{29} αααR (217)	37.7	D	
S/(S+R) (C_{29} ααα) (217)	0.44	M	0.55 (0.6%)
ββS/(ββS+ααR) (C29) (217)	0.59	M	0.70 (0.9%)
(C_{27}+C_{29})/(C_{27}+C_{28}+C_{29}) (217)	0.06		
C_{27}/C_{29} (αββS) (218)	0.85	D	
C_{28}/C_{29} (αββS) (218)	1.13	D	
Diaster/ααα Ster (C_{27}) (217)	2.06	M/D	1.00 (1.4%)
C30 αββS Sterane Index (218)	5.93	D	
C30 S+R Sterane Index (218)	5.86	D	
Terpanes (m/z 191)			
Oleanane/Hopane		D/A	
Gammacerane/Hopane	0.09	D	
Norhopane/Hopane	0.38	D	
Bisnorhopane/Hopane			
Diahopane/Hopane	0.14	M/D	
Moretane/Hopane	0.11	M	0.05 (0.7%)
25-nor-hopane/hopane		B	
Ts/(Ts+Tm) trisnorhopanes	0.83	M/D	1.00 (1.4%)
C29Ts/C29 Hopane	0.76	M	
H32 S/(R+S) Homohopanes	0.59	M	0.60 (0.6%)
H35/H34 Homohopanes	0.62	D	
C24 Tetracyclic/Hopane	0.05	D	
C24 Tetracyclic/C26 Tricyclics	0.22	D	
C23/C24 Tricyclic terpanes	1.17	D	
C19/C23 Tricyclic terpanes	0.10	D	
C26/C25 Tricyclic terpanes	1.12	D	
(C28+C29 Tricyclics)/Ts	2.01	A	
Various (m/z 191; 217)			
Steranes/Hopanes	0.93	D	
Tricyclic terpanes/Hopanes	0.43	M	1.00 (1.4%)
Tricyclic terpanes/Steranes	0.46	M/D	1.00 (1.4%)

[1]Definition and utility of the ratios can be found on our website www.BaselineDGSI.com
[2]A=Source Age; D=Depositional environment; M= Maturity; B=Possible Biodegradation
[3]Thermal equilibrium value of the biomarker ratio and in brackets the approximate VR value at which this value is reached

Figure 5.3 GC-MS Traces for Saturate Compounds

17

Table 5.2 Compounds detected in saturate GC-MS

Company:				Client ID:			
Well Name:				Project #:			
Depth:				Lab ID:			
Sampling Point:				File Name:			

Ion	Peak Label	Compound Name	Ret. Time	Area	Height	ppm (Area)	ppm (Hght)
217	CHOL	5β cholane (internal standard)	42.247	9466	1533	100.0	100.0
123	LABD	labdane					
123	RIMU	rimuane					
123	PIM	pimarane					
123	ENTBEY	ent-beyerane					
123	ISOPIM	isopimarane					
123	B_PHYLLO	β-phyllocladane					
123	B_KAUR	β-kaurane					
123	A_PHYLLO	α-phyllocladane					
125	BCAROT	β-carotane					
187	4MDIAM	4-methyldiamantane	9.294	65	26	0.7	1.7
187	1MDIAM	1-methyldiamantane	9.886	83	24	0.9	1.6
187	3MDIAM	3-methyldiamantane	10.252	55	19	0.6	1.2
188	DIAM	diamantane	9.137	75	29	0.8	1.9
191	TR19	C19 tricyclic terpane	18.861	359	74	3.8	4.8
191	TR20	C20 tricyclic terpane	21.702	821	149	8.7	9.7
191	TR21	C21 tricyclic terpane	25.048	1676	277	17.7	18.1
191	TR22	C22 tricyclic terpane	28.463	931	128	9.8	8.4
191	TR23	C23 tricyclic terpane	32.693	3633	611	38.4	39.9
191	TR24	C24 tricyclic terpane	35.082	3116	513	32.9	33.5
191	DESAOL	des-A-oleanane					
191	DESALU	des-A-lupane					
191	TR25A	C25 tricyclic terpane (a)	40.173	1997	292	21.1	19.0
191	TR25B	C25 tricyclic terpane (b)	40.312	1701	290	18.0	18.9
191	DESEHOP	des-E-hopane	43.433	925	147	9.8	9.6
191	TR26A	C26 tricyclic terpane (a)	44.061	1990	282	21.0	18.4
191	TR26B	C26 tricyclic terpane (b)	44.374	2159	324	22.8	21.1
191	TR28A	C28 tricyclic terpane (a)	53.005	2761	426	29.2	27.8
191	TR28B	C28 tricyclic terpane (b)	53.598	2952	411	31.2	26.8
191	TR29A	C29 tricyclic terpane (a)	55.550	2674	404	28.2	26.4
191	TR29B	C29 tricyclic terpane (b)	56.300	2706	449	28.6	29.3
191	TR30A	C30 tricyclic terpane (a)	60.519	2851	416	30.1	27.1
191	TR30B	C30 tricyclic terpane (b)	61.339	2769	432	29.3	28.2
191	TS	Ts 18α(H)-trisnorhopane	57.712	5520	872	58.3	56.9
191	TM	Tm 17α(H)-trisnorhopane	59.351	1118	168	11.8	11.0
191	H28	C28 17α18α21β(H)-bisnorhopane					
191	NOR25H	C29 Nor-25-hopane					
191	H29	C29 Tm 17α(H)21β(H)-norhopane	65.140	7135	1069	75.4	69.7
191	C29TS	C29 Ts 18α(H)-norneohopane	65.401	5425	749	57.3	48.9
191	DH30	C30 17α(H)-diahopane	66.151	2790	397	29.5	25.9
191	M29	C29 normoretane	67.110	1012	129	10.7	8.4
191	OL	oleanane					
191	H30	C30 17α(H)-hopane	68.609	19806	2981	209.2	194.5
191	M30	C30 moretane	70.196	2266	290	23.9	18.9

Table 5.2 Continued

Company:				Client ID:				
Well Name:				Project #:				
Depth:				Lab ID:				
Sampling Point:				File Name:				

Ion	Peak Label	Compound Name	Ret. Time	Area	Height	ppm (Area)	ppm (Hght)
191	H31S	C31 22S 17α(H) hopane	72.689	6936	1045	73.3	68.2
191	H31R	C31 22R 17α(H) hopane	73.194	7530	972	79.5	63.4
191	GAM	gammacerane	73.648	1777	213	18.8	13.9
191	H32S	C32 22S 17α(H) hopane	75.932	6063	887	64.1	57.9
191	H32R	C32 22R 17α(H) hopane	76.612	4190	573	44.3	37.4
191	H33S	C33 22S 17α(H) hopane	79.645	4047	584	42.8	38.1
191	H33R	C33 22R 17α(H) hopane	80.604	3124	421	33.0	27.5
191	H34S	C34 22S 17α(H) hopane	83.516	3001	394	31.7	25.7
191	H34R	C34 22R 17α(H) hopane	84.667	2202	284	23.3	18.5
191	H35S	C35 22S 17α(H) hopane	87.247	1874	284	19.8	18.5
191	H35R	C35 22R 17α(H) hopane	88.555	1354	195	14.3	12.7
205	H31_2ME	C31- 2α-methylhopane	68.975	605	91	6.4	5.9
205	H31S_205	C31 22S 17α(H) hopane	72.689	2134	327	22.5	21.3
205	H31R_205	C31 22R 17α(H) hopane	73.194	1627	220	17.2	14.4
205	H31_3ME	C31 3β-methylhopane					
217	S21	C21 sterane	29.021	3095	442	32.7	28.8
217	S22	C22 sterane	33.757	1483	230	15.7	15.0
217	DIA27S	C27 βα 20S diasterane	48.454	5524	821	58.4	53.6
217	DIA27R	C27 βα 20R diasterane	50.006	3795	548	40.1	35.7
217	DIA28SA	C28 βα 20S diasterane a	52.255	3791	547	40.0	35.7
217	DIA28SB	C28 βα 20S diasterane b	52.534	4708	580	49.7	37.8
217	DIA28RA	C28 βα 20R diasterane a	53.964	2761	391	29.2	25.5
217	DIA28RB	C28 βα 20R diasterane b	54.138	3387	406	35.8	26.5
217	C27S	C27 αα 20S sterane	55.149	2393	319	25.3	20.8
217	BB_D29S	C27 ββ 20R + C29 dia20S	55.672	8003	609	84.5	39.7
217	C27BBS	C27 ββ 20S sterane	56.073	4788	570	50.6	37.2
217	C27R	C27 αα 20R sterane	56.963	2126	272	22.5	17.7
217	DIA29R	C29 βα 20R diasterane	57.573	5539	482	58.5	31.4
217	C28S	C28 αα 20S sterane	59.281	2382	269	25.2	17.5
217	C28BBR	C28 ββ 20R sterane(+5 βαα)	60.014	5143	600	54.3	39.1
217	C28BBS	C28 ββ 20S sterane	60.415	5543	645	58.6	42.1
217	C28R	C28 αα 20R sterane	61.583	2558	196	27.0	12.8
217	C29S	C29 αα 20S sterane	62.786	2261	237	23.9	15.5
217	C29BBR	C29 ββ 20R sterane(+5 βαα)	63.605	4725	553	49.9	36.1
217	C29BBS	C29 ββ 20S sterane	63.937	4054	486	42.8	31.7
217	C29R	C29 αα 20R sterane	65.349	2836	237	30.0	15.5
218	C27ABBR	C27 ββ 20R sterane	55.655	6582	842	69.5	54.9
218	C27ABBS	C27 ββ 20S sterane	56.073	5260	726	55.6	47.4
218	C28ABBR	C28 ββ 20R sterane	60.014	6856	913	72.4	59.6
218	C28ABBS	C28 ββ 20S sterane	60.397	7005	922	74.0	60.1
218	C29ABBR	C29 ββ 20R sterane	63.605	6071	818	64.1	53.4
218	C29ABBS	C29 ββ 20S sterane	63.937	6179	779	65.3	50.8
218	C30ABBR	C30 ββ 20R sterane	66.639	1201	171	12.7	11.2
218	C30ABBS	C30 ββ 20S sterane	66.866	1163	152	12.3	9.9

Table 5.2 Continued

Company:	Client ID:
Well Name:	Project #:
Depth:	Lab ID:
Sampling Point:	File Name:

Ion	Peak Label	Compound Name	Ret. Time	Area	Height	ppm (Area)	ppm (Hght)
259	D27S	C27 βα 20S diasterane	48.454	3471	539	36.7	35.2
259	D27R	C27 βα 20R diasterane	50.006	2471	366	26.1	23.9
259	D28SA	C28 βα 20S diasterane a	52.255	2730	395	28.8	25.8
259	D28SB	C28 βα 20S diasterane b	52.534	3002	394	31.7	25.7
259	D28RA	C28 βα 20R diasterane a	53.964	2280	273	24.1	17.8
259	D28RB	C28 βα 20R diasterane b	54.155	1857	267	19.6	17.4
259	D29S	C29 βα 20S diasterane	55.759	4198	333	44.3	21.7
259	D29R	C29 βα 20R diasterane	57.590	2920	230	30.8	15.0
259	C30TP1	C30 tetracyclic polyprenoid	67.110	1886	269	19.9	17.5
259	C30TP2	C30 tetracyclic polyprenoid	67.267	1760	280	18.6	18.3

Table 5.3 Important ratios of detected saturate compounds

<table>
<tr><td>Company:</td><td>Client ID:</td></tr>
<tr><td>Well Name:</td><td>Project #:</td></tr>
<tr><td>Depth:</td><td>Lab ID:</td></tr>
<tr><td>Sampling Point:</td><td>File Name:</td></tr>
</table>

Miscellaneous Ratios	By Areas	By Heights
Steroids		
%C27 $\alpha\beta\beta$S (218)	28.5	29.9
%C28 $\alpha\beta\beta$S (218)	38.0	38.0
%C29 $\alpha\beta\beta$S (218)	33.5	32.1
C30 $\alpha\beta\beta$S Sterane Index (218)	5.9	5.9
C30 S+R Sterane Index (218)	5.9	6.1
C_{27}/C_{29} ($\alpha\beta\beta$S) (218)	0.85	0.93
C_{28}/C_{29} ($\alpha\beta\beta$S) (218)	1.13	1.18
C_{29}/C_{27} ($\alpha\beta\beta$S) (218)	1.17	1.07
%C27 $\alpha\alpha\alpha$R (217)	28.3	38.6
%C28 $\alpha\alpha\alpha$R (217)	34.0	27.8
%C29 $\alpha\alpha\alpha$R (217)	37.7	33.6
S/R (C_{29} $\alpha\alpha\alpha$) (217)	0.80	1.00
S/(S+R) (C_{29} $\alpha\alpha\alpha$) (217)	0.44	0.50
$\beta\beta/(\alpha\alpha+\beta\beta)$ (C_{29}) (217)	0.63	0.69
$\alpha\beta\beta$S/$\alpha\alpha\alpha$R (C_{29}) (217)	1.43	2.05
$(C_{21}+C_{22})/(C_{27}+C_{28}+C_{29})$ (217)	0.06	0.08
Diaster/$\alpha\alpha\alpha$ Ster (C_{27}) (217)	2.06	2.32
Terpenoids		
C19/C23 Tricyclic terpanes	0.10	0.12
C23/C24 Tricyclic terpanes	1.17	1.19
C26/C25 Tricyclic terpanes	1.12	1.04
C24 Tetracyclic/C26 Tricyclics	0.22	0.24
C24 Tetracyclic/Hopane	0.05	0.05
Ts/Tm trisnorhopanes	4.94	5.19
Ts/(Ts+Tm) trisnorhopanes	0.83	0.84
C29Ts/C29 Hopane	0.76	0.70
Bisnorhopane/Hopane		
Norhopane/Hopane	0.36	0.36
Diahopane/Hopane	0.14	0.13
Oleanane/Hopane		
Gammacerane/Hopane	0.09	0.07
Moretane/(Moretane+Hopane)	0.10	0.09
H32 S/(S+R) Homohopanes	0.59	0.61
H35/H34 Homohopanes	0.62	0.71
[Steranes]/[Hopanes]	0.93	0.74
[Tricyclic terpanes]/[Hopanes]	0.43	0.46
[Tricyclic terpanes]/[Steranes]	0.46	0.62

Figure 5.4 GC-MS Traces for Aromatic Compounds

Table 5.4 Compounds detected in aromatic GC-MS

Company:				Client ID:			
Well Name:				Project #:			
Depth:	-			Lab ID:			
Sampling Point:				File Name:			

Ion	Peak Label	Compound Name	Ret. Time	Area	Height	ppm (Area)	ppm (Hght)
230	OTP	*Ortho-terphenyl* (internal standard)	34.047	35661	11363	300.0	300.0
128	NAPH	Naphthalene	14.146	78237	26435	658.2	697.9
134	ISOR	Isorenieratane					
142	2MN	2-Methylnaphthalene	17.492	250883	82371	2110.6	2174.7
142	1MN	1-Methylnaphthalene	17.962	208532	64546	1754.3	1704.1
154	BP	Biphenyl	19.914	22377	7154	188.2	188.9
156	2EN	2-Ethylnaphthalene	20.506	33633	9875	282.9	260.7
156	1EN	1-Ethylnaphthalene	20.559	5454	3422	45.9	90.3
156	26DMN	2,6-Dimethylnaphthalene	20.855	133655	39156	1124.4	1033.8
156	27DMN	2,7-Dimethylnaphthalene	20.925	105214	39388	885.1	1039.9
156	1317DMN	1,3 & 1,7-Dimethylnaphthalenes	21.308	270963	88478	2279.5	2336.0
156	16DMN	1,6-Dimethylnaphthalene	21.413	247104	83914	2078.8	2215.5
156	2314DMN	2,3 & 1,4-Dimethylnaphthalenes	21.901	93804	24778	789.1	654.2
156	15DMN	1,5-Dimethylnaphthalene	21.970	56949	21064	479.1	556.1
156	12DMN	1,2-Dimethylnaphthalene	22.336	40076	13224	337.1	349.1
168	2MBP	2-Methylbiphenyl	20.576	7839	2766	65.9	73.0
168	DPM	Diphenylmethane	21.430	1260	378	10.6	10.0
168	3MBP	3-Methylbiphenyl	23.103	25967	8424	218.4	222.4
168	4MBP	4-Methylbiphenyl	23.382	12068	4030	101.5	106.4
168	DBF	Dibenzofuran	24.096	2698	795	22.7	21.0
170	BB_EMN	Ethyl-methyl-Naphthalene	23.870	61046	16515	513.6	436.0
170	AB_EMN	Ethyl-methyl-Naphthalene	24.358	31015	9916	260.9	261.8
170	137TMN	1,3,7-Trimethylnaphthalene	24.515	115638	38859	972.8	1025.9
170	136TMN	1,3,6-Trimethylnaphthalene	24.671	180895	54874	1521.8	1448.8
170	146135T	(1,4,6+1,3,5)-Trimethylnaphthalenes	25.125	154965	46505	1303.7	1227.8
170	236TMN	2,3,6-Trimethylnaphthalene	25.246	109008	35833	917.0	946.0
170	127TMN	1,2,7-Trimethylnaphthalene	25.560	36000	12176	302.9	321.5
170	167126T	(1,6,7+1,2,6)-Trimethylnaphthalenes	25.630	136474	30203	1148.1	797.4
170	124TMN	1,2,4-Trimethylnaphthalene	26.066	14717	4788	123.8	126.4
170	125TMN	1,2,5-Trimethylnaphthalene	26.275	39291	13182	330.5	348.0
178	PHEN	Phenanthrene	31.363	118452	34805	996.5	918.9
178	ANTH	Anthracene	31.625	2253	595	19.0	15.7
184	1357	1,3,5,7-Tetramethylnaphthalene	28.070	41744	9821	351.2	259.3
184	1367	1,3,6,7-Tetramethylnaphthalene	28.697	59872	19972	503.7	527.3
184	1247	(1,2,4,7+1,2,4,6+1,4,6,7)-Tetramethylnaphthalenes	29.115	48738	15972	410.0	421.7
184	1257	1,2,5,7-Tetramethylnaphthalene	29.220	22786	7495	191.7	197.9
184	2367	2,3,6,7-Tetramethylnaphthalene	29.446	10439	3289	87.8	86.8
184	1267	1,2,6,7-Tetramethylnaphthalene	29.673	18634	5815	156.8	153.5
184	1237	1,2,3,7-Tetramethylnaphthalene	29.777	6407	2033	53.9	53.7
184	1236	1,2,3,6-Tetramethylnaphthalene	29.952	11114	3648	93.5	96.3
184	1256	1,2,5,6-Tetramethylnaphthalene	30.370	14270	4098	120.0	108.2
184	DBT	Dibenzothiophene	30.614	12686	3808	106.7	100.5
191	BH32	C32 Benzohopane	64.816	830	196	7.0	5.2
191	BH33	C33 Benzohopane	66.264	1039	195	8.7	5.1
191	BH34	C34 Benzohopane	67.513	239	66	2.0	1.7
191	BH35	C35 Benzohopane					
192	3MP	3-Methylphenanthrene	34.361	64835	20042	545.4	529.1
192	2MP	2-Methylphenanthrene	34.483	68151	20746	573.3	547.7
192	9MP	9-Methylphenanthrene	34.953	105504	31525	887.6	832.3
192	1MP	1-Methylphenanthrene	35.075	82677	25261	695.5	666.9

Table 5.4 Continued

Company:		Client ID:					
Well Name:		Project #:					
Depth:	-	Lab ID:					
Sampling Point:		File Name:					

Ion	Peak Label	Compound Name	Ret. Time	Area	Height	ppm (Area)	ppm (Hght)
198	CAD	Cadalene					
198	12467PMN	1,2,4,6,7-Pentamethylnaphthalene	32.862	6791	2053	57.1	54.2
198	12357PMN	1,2,3,5,7-Pentamethylnaphthalene	33.071	3210	980	27.0	25.9
198	4MDBT	4 Methyl Dibenzothiophene	33.333	25187	7439	211.9	196.4
198	12367PMN	1,2,3,6,7-Pentamethylnaphthalene	33.733	3255	1031	27.4	27.2
198	23MDBT	2 & 3 Methyl Dibenzothiophenes	33.803	9519	2853	80.1	75.3
198	12356PMN	1,2,3,5,6-Pentamethylnaphthalene	34.204	2213	669	18.6	17.7
198	1MDBT	1 Methyl Dibenzothiophene	34.343	6574	1867	55.3	49.3
206	36DMP	3,6-Dimethylphenanthrene	37.126	14324	4882	120.5	128.9
206	26DMP	2,6-Dimethylphenanthrene	37.326	26594	8448	223.7	223.0
206	27DMP	2,7-Dimethylphenanthrene	37.398	14016	4455	117.9	117.6
206	39DMP	(3,9+3,10+2,10+1,3)-Dimethylphenanthrenes	37.742	156191	41510	1314.0	1095.9
206	29DMP	(2,9+1,6)-Dimethylphenanthrenes	37.905	76761	16870	645.8	445.4
206	17DMP	1,7-Dimethylphenanthrene	38.013	53985	17094	454.2	451.3
206	23DMP	2,3-Dimethylphenanthrene	38.194	20817	6023	175.1	159.0
206	19DMP	1,9-Dimethylphenanthrene	38.267	34485	10390	290.1	274.3
206	18DMP	1,8-Dimethylphenanthrene	38.574	18366	5303	154.5	140.0
206	12DMP	1,2-Dimethylphenanthrene	38.936	10049	3091	84.5	81.6
219	RET	Retene	41.940	3613	777	30.4	20.5
231	231A20	C20 Triaromatic Steroid	46.411	12185	3824	102.5	101.0
231	231B21	C21 Triaromatic	48.275	9726	2674	81.8	70.6
231	231C26	C26 20S Triaromatic	54.989	2960	770	24.9	20.3
231	231D26	C27 20S & C26 20R Triaromatic	56.147	10720	2954	90.2	78.0
231	231E28	C28 20S Triaromatic	57.088	8387	1841	70.6	48.6
231	231F27	C27 20R Triaromatic	57.541	6930	1655	58.3	43.7
231	C29TA1	C29 Triaromatic	57.794	1408	328	11.8	8.7
231	C29TA2	C29 Triaromatic	57.939	688	192	5.8	5.1
231	231G28	C28 20R Triaromatic	58.663	7351	1783	61.8	47.1
231	DINO	Triaromatic Dinosteroid	58.735	896	434	7.5	11.5
231	TA_OL	Triaromatic Oleanoid					
231	C29TA3	C29 Triaromatic	59.586	1631	331	13.7	8.7
245	C3S	C27 20S 3-Methyl Triaromatic Steroid	56.907	827	205	7.0	5.4
245	C4S	C27 20S 4-Methyl Triaromatic Steroid	57.342	696	181	5.9	4.8
245	E2S	C28 20S 2-Methyl Triaromatic Steroid	57.740	570	193	4.8	5.1
245	E3SC3R	C28 20S 3-Methyl & C27 20R 3-Methyl TAS	57.993	3614	876	30.4	23.1
245	E4SC4R	C28 20S 4-Methyl & C27 20R 4-Methyl TAS	58.409	2691	568	22.6	15.0
245	S2S	C29 20S 2-Methyl Triaromatic Steroid	58.590	829	192	7.0	5.1
245	DA	Triaromatic Dinosteroid a	58.771	1134	289	9.5	7.6
245	S3S	C29 20S 3-Methyl Triaromatic Steroid	58.862	3042	562	25.6	14.8
245	DB	Triaromatic Dinosteroid b	59.170	1451	349	12.2	9.2
245	S4SE2R	C29 20S 4-Methyl & C28 20R 2-Methyl TAS	59.278	3003	597	25.3	15.8
245	E3R	C28 20R 3-Methyl Triaromatic Steroid	59.369	3413	670	28.7	17.7
245	E4R	C28 20R 4-Methyl Triaromatic Steroid	59.785	1924	395	16.2	10.4
245	DC	Triaromatic Dinosteroid c	59.930	1643	354	13.8	9.3
245	DD	Triaromatic Dinosteroid d	60.002	1483	405	12.5	10.7
245	S2R	C29 20R 2-Methyl Triaromatic Steroid	60.292	1147	205	9.6	5.4
245	S3R	C29 20R 3-Methyl Triaromatic Steroid	60.454	2996	689	25.2	18.2
245	DE	Triaromatic Dinosteroid e	60.563	1845	334	15.5	8.8
245	S4R	C29 20R 4-Methyl Triaromatic Steroid	60.889	1861	438	15.7	11.6
245	DF	Triaromatic Dinosteroid f	60.979	2167	481	18.2	12.7

Tables 5.4 Continued

Company:		Client ID:
Well Name:		Project #:
Depth:		Lab ID:
Sampling Point:		File Name:

Ion	Peak Label	Compound Name	Ret. Time	Area	Height	ppm (Area)	ppm (Hght)
253	S253A	C21 Ring-C Monoaromatic Steroid	40.656	6218	1359	52.3	35.9
253	S253B	C22 Monoaromatic steroid	42.447	3150	767	26.5	20.3
253	S253C	C27 Reg 5β(H),10β(CH3) 20S	49.813	785	229	6.6	6.0
253	S253D	C27 Dia 10β(H),5β(CH3) 20S	49.903	2124	599	17.9	15.8
253	S253E	C27 Dia10βH,5βCH3 20R+Reg5βH,10βCH3 20R	51.007	2138	536	18.0	14.2
253	S253F	C27 Reg 5α(H),10β(CH3) 20S	51.116	1307	368	11.0	9.7
253	S253G	C28 Dia 10αH,5αCH3 20s+Reg5βH,10βCH3 20S	51.424	4243	973	35.7	25.7
253	S253H	C27 Reg 5α(H),10β(CH3) 20R	52.365	1619	308	13.6	8.1
253	S253I	C28 Reg 5α(H),10β(CH3) 20S	52.491	1633	433	13.7	11.4
253	S253J	C28 Dia 10αH,5αCH3 20R+Reg5βH,10βCH3 20R	52.618	3415	853	28.7	22.5
253	S253K	C29 Dia 10βH,5βCH3 20S+Reg5βH,10βCH3 20S	52.727	3104	719	26.1	19.0
253	S253L	C29 Reg 5α(H),10β(CH3) 20S	53.668	2827	653	23.8	17.2
253	S253M	C28 Reg 5α(H),10β(CH3) 20R	53.867	2307	519	19.4	13.7
253	S253N	C29 Dia 10βH,5βCH3 20R+Reg5βH,10βCH3 20R	53.939	2993	568	25.2	15.0
253	PERYLENE	Perylene					
253	S253O	C29 Reg 5α(H),10β(CH3) 20R	55.116	1799	334	15.1	8.8
342	OHTMP	C26 Octahydrotetramethylpicene					
365	SH29	C29 8,14-secohopanoids	55.061	8272	2414	69.6	63.7
365	SH30	C30 8,14-secohopanoids	56.491	8141	2173	68.5	57.4

Table 5.5 Important ratios of detected aromatic compounds

Company:		Client ID:	
Well Name:		Project #:	
Depth:		Lab ID:	
Sampling Point:		File Name:	

Miscellaneous Ratios	By Areas	By Heights
Triaromatic Steroids m/z 231		
(C20+C21)/Σ TAS	0.37	0.41
TAS #1 20/20+27	0.64	0.70
TAS #2 21/21+28	0.57	0.60
%26TAS	15.7	17.0
%27TAS	36.7	36.5
%28TAS	39.0	39.3
%29TAS	8.6	7.3
C28/C26 20S TAS	2.83	2.39
C28/C27 20R TAS	1.06	1.08
Monoaromatic Steroids m/z 253		
Dia/Regular C27 MAS	2.71	2.62
%27 MAS	26.3	28.8
%28 MAS	38.3	39.2
%29 MAS	35.4	32.1
(C21+C22)/Σ MAS	0.24	0.23
TAS/(MAS+TAS)	0.60	0.63
TA28/(TA28+MA29)	0.59	0.61
Triaromatic Methylsteroids m/z 245		
Dinosteroid Index	0.27	0.28
C4/C3+C4 Mester	0.38	0.39
Phenanthrenes and Naphthalenes		
MPI-1	0.65	0.67
MPI-2	0.67	0.68
Rc(a) if Ro < 1.3 (Ro%)	0.76	0.77
Rc(b) if Ro > 1.3 (Ro%)	1.91	1.90
DNR-1	4.19	3.73
DNR-2	2.55	3.17
TNR1	0.70	0.77
TDE-1	2.67	2.75
TDE-2	0.26	0.40
MDR	3.83	3.98
Rm (Ro%)	0.79	0.80
MDR23	0.75	0.75
MDR1	0.52	0.49
DBT/Phenanthrene	0.11	0.11
New Ratios		
PNR	0.75	0.75
MDPNR	0.73	0.72
Dinosteroid Index 2	0.11	0.20

5.3 Results through Different Geological Time

The following figures (Figures 5.5 to 5.15, listed in the order of geological time) are results of tested oil samples by GeoMark Research, Inc. published in Peters et al. (2005).These results will help explain some theories on biomarkers, and will also be used to discuss and explain biomarkers further by comparing and contrasting the values with results of my Eagle Ford sample.

Figure 5.5 Precambrian Iremeken shale formation showing whole oil GC and saturate compound GC-MS traces with important values/ratios (Peters et al., 2005)

28

Figure 5.6 Cambrian Huqf Supergroup showing whole oil GC and saturate compound GC-MS traces with important values/ratios (Peters et al., 2005)

Figure 5.7 Ordovician Red River formation showing whole oil GC and saturate compound GC-MS traces with important values/ratios (Peters et al., 2005)

Figure 5.8 Lower Silurian Qusaiba shale showing whole oil GC and saturate compound GC-MS traces with important values/ratios (Peters et al., 2005)

Figure 5.9 Devonian Lacustrine Old Red sandstone formation showing whole oil GC and
saturate compound GC-MS traces with important values/ratios (Peters et al., 2005)

Figure 5.10 Mississippian Woodford shale showing whole oil GC and saturate compound GC-MS traces with important values/ratios (Peters et al., 2005)

Figure 5.11 Permian Phosphoria carbonate formation showing whole oil GC and saturate compound GC-MS traces with important values/ratios (Peters et al., 2005)
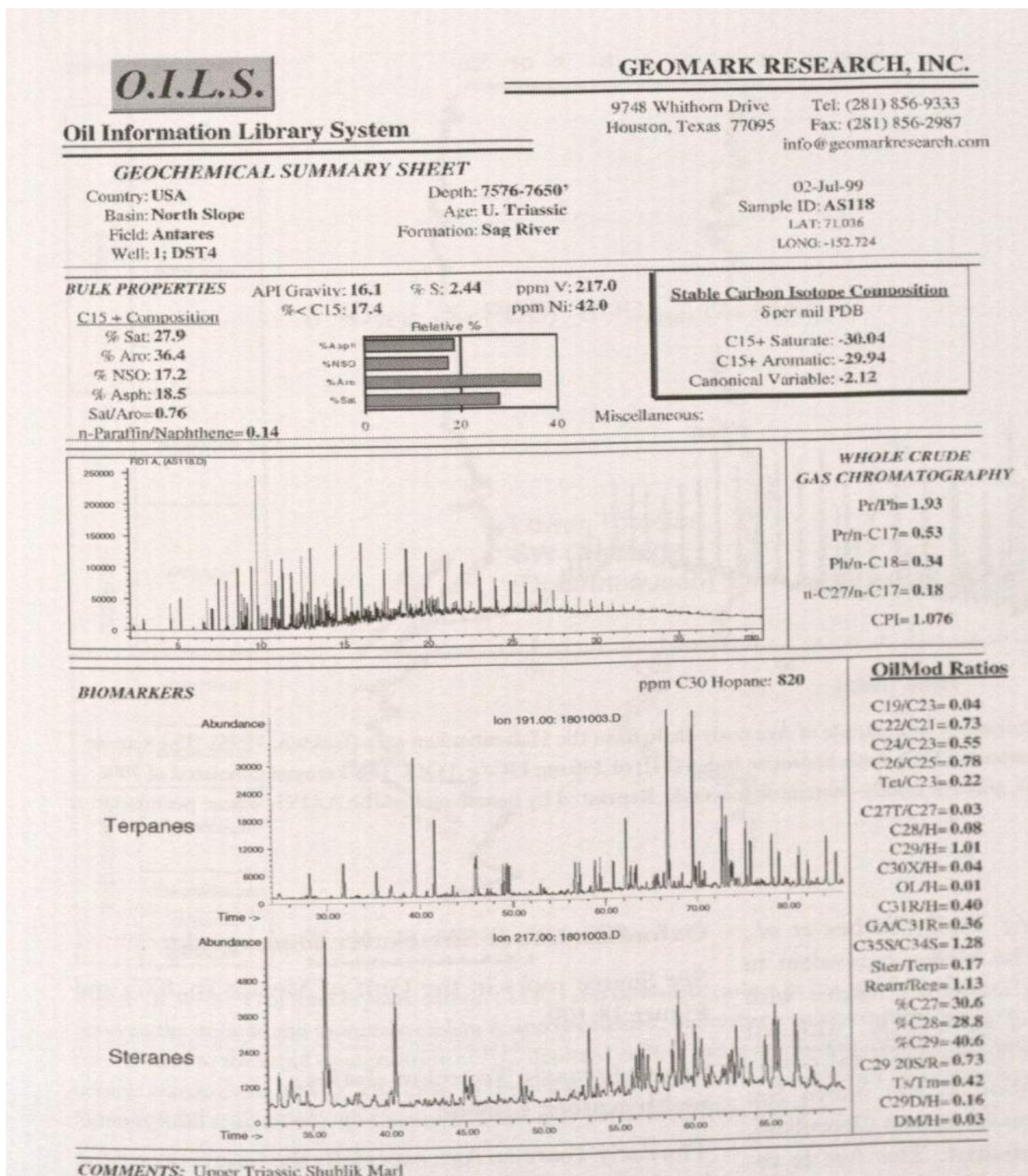
Figure 5.12 Triassic Shublik formation showing whole oil GC and saturate compound GC-MS
traces with important values/ratios (Peters et al., 2005)
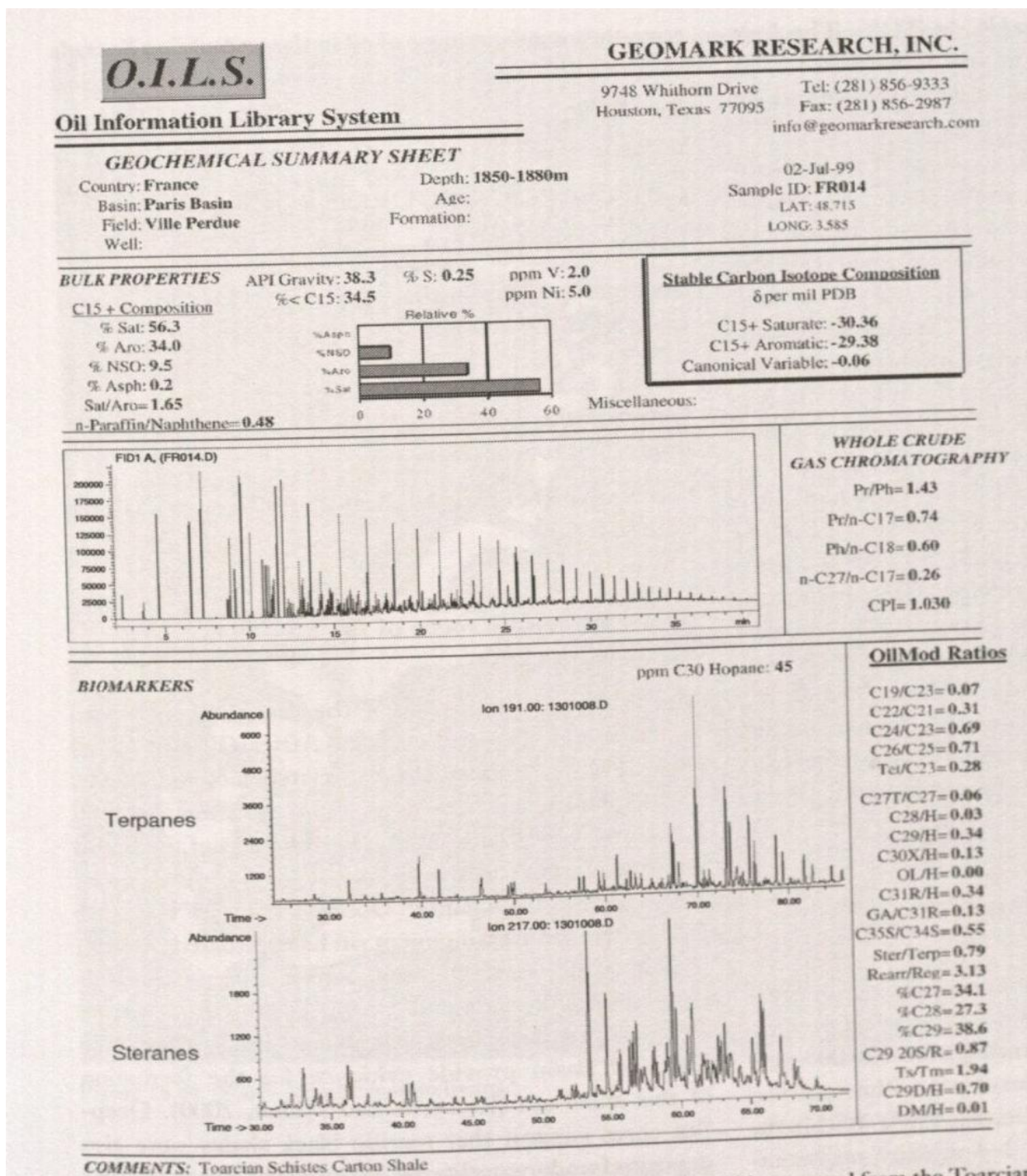
Figure 5.13 Jurassic Toarcian Schistes Carton shale showing whole oil GC and saturate compound GC-MS traces with important values/ratios (Peters et al., 2005)

Figure 5.14 Cretaceous Iabe formation showing whole oil GC and saturate compound GC-MS traces with important values/ratios (Peters et al., 2005)

Figure 5.15 Tertiary (Miocene) Heath shale formation showing whole oil GC and saturate compound GC-MS traces with important values/ratios (Peters et al., 2005)

CHAPTER 6

DISCUSSION

<u>6.1 Application of Biomarkers in Age Dating</u>

The process of using biomarkers for age dating is primarily based on the taxa that formed the biomarker: therefore the source-organism of a biomarker needs to be known or else the age of oil cannot be known by the biomarker alone. Other clues like the known source of a reservoir can be used to support the biomarker in cases where the age dating from biomarker(s) is not conclusive. Table 6.1 shows biomarkers, the related organism, and the age range when the taxa were abundant. Figure 6.1 complements Table 6.1, both figure and table were compiled from various papers (Grantham and Wakefield, 1988; Moldowan et al., 1994; Moldowan et al., 1996; Holba et al., 1998; Moldowan, 2000; Moldowan and Jacobson, 2000; Moldowan et al., 2001; Holba et al., 2001)

Table 6.1 Suggested age-related biomarkers (Peters et al., 2005)

Biomarker or biosignature	Related (main) organisms	Age range for high abundance	Other limitations
nC_{15}, nC_{17}, nC_{19}	*G. prisca*	Cambrian–Devonian	–
Botryococcane	*B. braunii*	Only known in Tertiary	Lacustrine, rare
24–Isopropylcholestane	Porifera (class Demospongiae)	Abundant in some Vendian–Ordovician	Marine
Oleananes, lupanes	Angiosperms	Cretaceous or younger, higher in some Tertiary	Rare in pre-Cretaceous
Dinosterane, triaromatic dinosteroids	Dinoflagellates	Abundant in some Triassic or younger	Abundant in some Paleozoic-Precambrian
Triaromatic 23,24–dimethylcholesteroids	Haptophytes, dinoflagellates	Common in Triassic or younger	Rare in Paleozoic
24–Norcholestane, 24–nordiacholestanes	Diatoms?	Abundant in some Cretaceous or younger, higher in some Tertiary	Maximum effect at high latitudes, verified only for oils
C_{20}, C_{25}, C_{30} highly branched isoprenoids	Diatoms	Cretaceous or younger	Few data
C_{28}–C_{29} tricyclic terpane/18α–22,29, 30–trisnorneohopane (Ts)	Green algae?, bacteria	Decreases from Upper Triassic to Upper Jurassic	Few Phanerozoic data
Baccharane	Unknown	Triassic rocks (Adriatic)	Rare
C_{28}/C_{29} steranes	Algae	Increases from Precambrian-Tertiary	Marine settings without terrigenous input
Beyerane, kaurane, phyllocladane	Terrigenous plants	Devonian and younger	Few data
Cadinanes	Terrigenous plants	Jurassic and younger, present to at least Permian	Few data
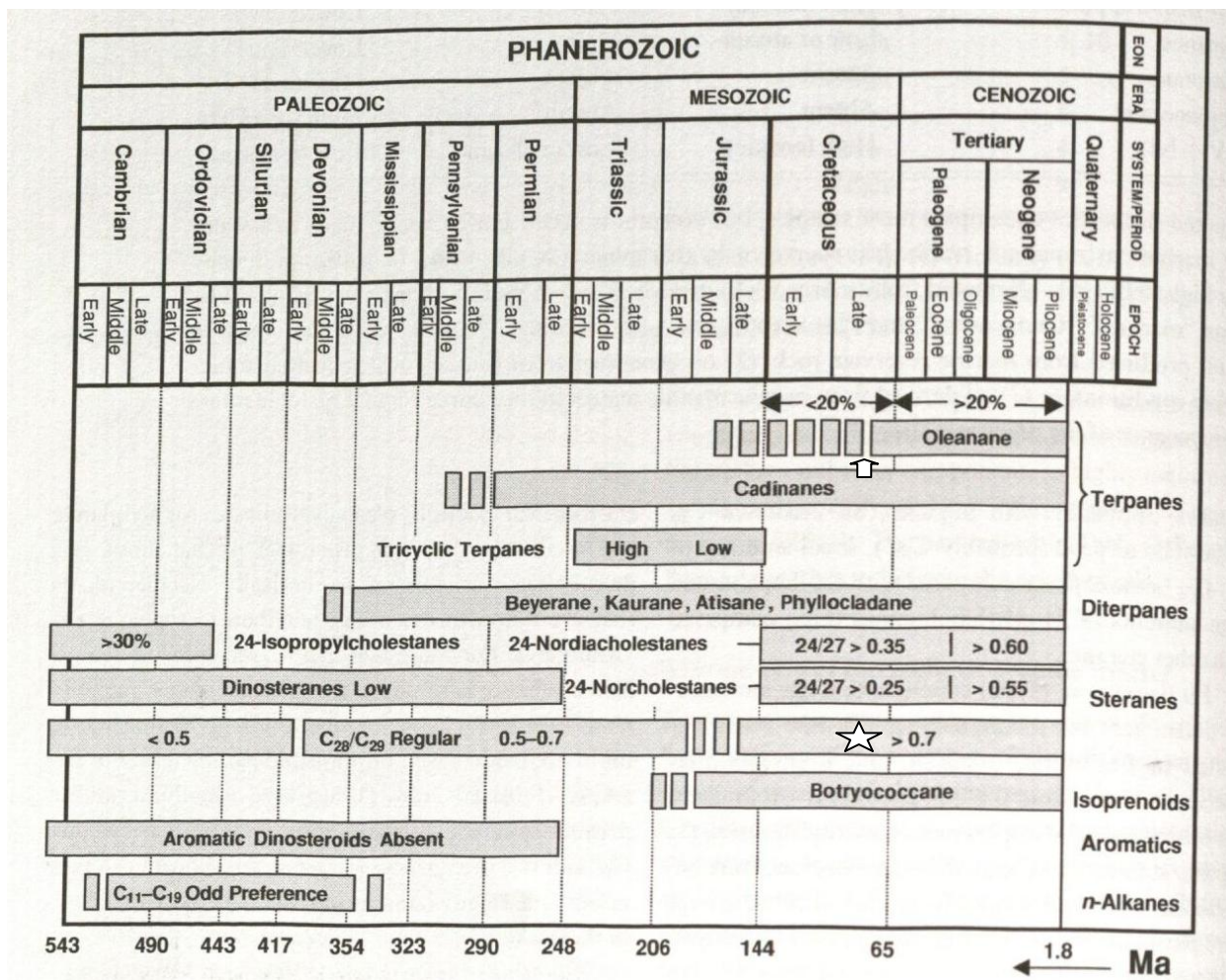
Figure 6.1 Age-related parameters of the source rock (Peters et al., 2005).
The arrow and star symbol indicate the results of my Eagle Ford sample.

Figure 6.1 and Table 6.1 are partially supported by the results in Section 5. The ratio of

C28/C29 steranes increases through time: the ratio of C28/C29 in Figures 9, 14 and 19 are 0.3,

0.5 and 1.47 respectively. My results of Eagle Ford oil sample support Figure 6.1 as well, using

results on steranes from Figure 5.3 and using the m/z 217. The C28/C29 ratio of 34 over 37.7 is

0.9 (☆) which falls into the category of Cretaceous or younger in Figure 6.1.

The presence of the biomarker oleanane is inconsistent; does not occur, or is less than 20% when it does occur prior to the Tertiary period according to Figure 6.1. Section 5 results support this theory; Figure 5.14 having oleanane value of or 80% strongly suggests the presence of angiosperms during deposition. The lack of oleanane values in my saturate GC-MS result supports the inconsistencies of oleanane (⌂) during the Cretaceous period. In my result (Figure 5.3) the ratio of (C28+C29 Tricyclics)/Ts is 2.01 (low) Holba et al. (2001) stated that values of >2 are high and <2 are low (Jurassic in age or younger). The presence of dinosteroid in my results (Dinosteroid index on Figure 5.4) suggest Triassic or younger on Figure 6.1. These interpretations narrow the age down to Cretaceous period. My results on the Eagle Ford formation lack values for some biomarkers on Figure 6.1 due to variables like the m/z of GC-MS.

<u>6.2 Application of Biomarker in Determining the Depositional Environment</u>

The usage of biomarkers to determine the depositional environment is more common than using it in age dating. The "D"s (depositional environment) on the ratios in Figure 5.3 and 5.4 show how many more biomarkers are used for D over "A" for age dating. This is mainly because there is more information about biological origins' habitant than its age of abundance for biomarkers. Table 6.1 above shows the main organism of the biomarkers mentioned, although Tables 6.2 and 6.3 do not give the main organisms for the biomarkers, both tables give the inferred depositional environment.

Table 6.2 Parameters of carbonate versus shale source rocks (Peters et al., 2005)

Characteristics	Shales	Carbonates	References
Non-biomarker parameters			
API, gravity	Medium–high	Low–medium	1, 2, 3
Sulfur, wt.%	Variable	High (marine)	1, 2, 3, 6, 9
Thiophenic sulfur	Low	High	1
Saturate/aromatic	Medium–high	Low–medium	1, 2, 3
Naphthenes/alkanes	Medium–low	Medium–high	1, 3
Carbon preference index (C_{22}–C_{32})	≥ 1	≤ 1	1, 2, 6, 9
Biomarker parameters			
Pristane/phytane	High (≥ 1)	Low (≤ 1)	1, 2, 6, 9, 10
Phytane/nC_{18}	Low (≤ 0.3)	High (≥ 0.3)	2, 6
Steranes/17α-hopanes	High	Low	7, 9
Diasteranes/steranes	High	Low	1
C_{24} tetra-/C_{26} tricyclic diterpanes	Low–medium	Medium–high	2, 7
C_{29}/C_{30} hopane	Low	High (>1)	10, 11
C_{35} homohopane index	Low	High	4, 10
Hexahydrobenzohopanes and benzohopanes	Low	High	5
Dia/(Reg + Dia) monoaromatic steroids	High	Low	8
Ts/(Ts + Tm)	High	Low	4
C_{29} monoaromatic steroids	Low	High	9

References: (1) Hughes (1984), (2) Palacas (1984), (3) Tissot and Welte (1984), (4) McKirdy *et al.* (1983), (5) Connan and Dessort (1987), (6) Connan (1981), (7) Connan *et al.* (1986), (8) Riolo *et al.* (1986), (9) Moldowan *et al.* (1985), (10) ten Haven *et al.* (1988), (11) Fan Pu *et al.* (1987).

Table 6.3 Parameters based on the organic matter from marine, terrigenous, and lacustrine
source rock (Peters et al., 2005)

Property	Marine	Terrigenous	Lacustrine
Sulfur (wt.%)	High (anoxic)	Low	Low
C_{21}–C_{35} n-alkanes	Low	High	High
Pristane/phytane	<2	>3	~1–3
Pristane/nC_{17}	Low (<0.5)	High (>0.6)	–
4-Methylsteranes	Moderate	Low	High
C_{27}–C_{29} steranes	High C_{28}	High C_{29}	High C_{27}
C_{30} 24-n-propylcholestane	Low	Low or absent	Absent
Steranes/hopanes	High	Low	Low
Bicyclic sesquiterpanes	Low	High	Low
Tricyclic diterpanes	Low	High	High
Tetracyclic diterpanes	Low	High	Low
Lupanes, bisnorlupanes	Low	High	Low
28,30-Bisnorhopane	High (anoxic)	Low	Low
Oleananes	Low or absent	High	Low
β-Carotane	Absent	Absent	High (arid)
Botryococcane	Absent	Absent	High (brackish)
V/(V + Ni)	High (anoxic)	Low or absent	Low or absent

The following are derived from my oil sample results in section 5.2 and are highlighted in tables 7 and 8: pristane/phytane is 1.53; diasteranes/steranes is 2.06 (high); C24 tetracyclic/C26 tricyclics is 0.22 (low); steranes/hopanes ~ 1(high); and Oleananes is absent. Using both tables 7 and 8 as a guide to interpret my results, the oil sample of the Eagle Ford formation is from a shale source rock and a marine depositional environment. Some biomarkers in my results do not fully support this depositional environment, but they also do not fully support other depositional environments. These biomarkers lay in the grey area of the parameters mentioned in the tables above. For example, in Table 6.3 C27-C29 steranes has a relatively high C28 in marine environments. In my results (Figure 5.4/Table 4.5) C28 is higher than C29 in m/z 218 but is less in m/z 217. Further investigation led me to the paper of Philp et al. (1989) where it stated that C28 and C29 are higher than C27 in the marine environment,

suggesting that the slight discrepancy does not discount my sample as being from a marine environment.

The depositional environments of the oil samples in Section 5.3 can also be supported by the biomarker values using the parameters in Tables 6.1 and 6.2 as a guide.

- Fig. 5.5 Precambrian Iremeken formation is shale environment (Filiptsov et al., 1999) and the biomarker results show: a high API gravity of 40.2 (shale); high saturate/aromatic (shale); carbon preference index >1(shale); a value of 0.87 (a medium-high value, so cannot fully suggest "carbonates") for the ratio of pristane/phytane (marine); pristine/nC17 is 0.15 (marine).

- Fig. 5.6 Early Cambrian Huqf formation is a carbonate source rock (Grantham et al., 1988; Pollastro, 1999; Terken et al., 2001) and the results show: low API gravity (carbonate); low saturate/aromatic value (carbonate); low pristane/phytane (carbonate).

- Fig. 5.7 Ordovician Red River formation is a marine shale (Hatch et al., 1987; Pancost et al., 1999) and the results show: high API gravity (shale); CPI >1 (shale); C29/hopane is low~0.53 (shale); pristine/nC17 is 0.06 (marine); pristane/phytane <2 (marine).

- Fig. 5.8 Lower Silurian Qusaiba Shale is part of a source unit that occurs across the northern African and Arabian cratons (Cole et al., 1994a; Cole et al., 1994b; Jones and Stump, 1999; Tissot et al., 1984), and the depositional environment was marine (Tyson, 1995). The results show: high API gravity value, high saturate/aromatic value, and high pristane/phytane value (shale); oleane/hopane is 0 (marine).

- Fig. 5.9 There are uncertainties as to the source rock of this oil, but the favored theory is that the majority of oil originated from the Devonian Lacustrine Old Red sandstone formation (Peters et al., 1989; Peters et al., 1999). Another

theory is that the source is Devonian shale with marine incursions (Bailey et al., 1990; Marshall, 1996). The results show: high API gravity, high saturate/aromatic, pristane/phytane (shale); pristane/phytane 2.17 (lacustrine); low oleananes (marine and lacustrine).

- Fig. 5.10 The Mississippian Woodford shale is a marine/anoxic (Lambert, 1993; Lambert et al., 1994; Wang and Philip, 1997) shale source rock (Lewan, 1983; Michels et al., 1995; Montgomery, 1990). The results show: pristane/phytane is 1.37 (marine and shale); high API gravity and high saturate/aromatic (shale).

- Fig. 5.11 Permian Phosphoria formation was deposited in an environment that favored cyclic anoxia (marine) and salinity stratification (Dahl et al., 1993). The formation is mainly shale (Parrish, 1982; Maughan, 1993; Jewell, 1995). However, the oil sample in the results was taken from a carbonate layer in the formation (Peters et al., 2005), so the results would have conflicting properties for different biomarkers. The result show: medium API gravity (carbonate); low saturate/aromatic (carbonate); pristane/phytane id 0.71 (marine and carbonate); pristane/nC17 is 0.39 (marine).

- Fig. 5.12 The Shublik formation consists of marine carbonate, marl and phosphorite in a transgressive, upwelling depositoinal environment (Kupecz, 1995). The test sample was from the marl (carbonate). The results show: low API gravity and saturate/aromatic (carbonate); high sulfur wt.% (marine carbonate); low oleananes (marine).

- Fig. 5.13 The Schistes Carton is a marine shale source rock (Espitalie et al., 1987; Katz, 1995; Disnar et al., 1996). The results show: high API gravity and saturate/aromatic (shale); pristane/phytane is 1.43 (marine and shale); oleananes is absent (marine).

- Fig. 5.14 The Iabe is a marine shale source rock in the offshore Congo Delta (Burwood, 1999; Cole et al., 2000; Schoellkopf and Patterson, 2000). The results show: pristane/phytane is 1.23 (marine and shale).

- Fig. 5.15 The source rock of this oil sample is the Miocene Heath formation and it is marine shale (Higley, 2002). The results show: pristane/phytane is 1.59 (marine and shale); high saturate/aromatic (shale); low C29/(C30)hopane value (shale).

<u>6.3 Application of Biomarkers in Determining Thermal Maturity</u>

Thermal maturity is caused by time and temperature and not the amount of petroleum generated (Peters and Moldowan, 1993), therefore, it is wrong to conclude that a reservoir/source rock will "dry up" based on how much production has occurred. This is why figuring out the thermal maturity is important for exploration purposes. The basic explanation of how biomarkers can be used to determine thermal maturity is by obtaining a ratio of two biomarkers that deteriorate inversely (or at different rates) due to thermal maturity. Both biomarkers need to have similar properties for the effect of time and temperature to have similar effects on the biomarkers. An example of biomarkers used in determining thermal maturity is the ratio of moretanes/hopanes, both biomarkers decrease relative to each other with thermal maturity due to their chemical properties (Seifert and Moldowan, 1980). The ratio value of moretanes/hopanes for mature oils ranges from 0.05 to 0.15 (Mackenzie et al., 1980; Seifert and Moldowan, 1980). The value for the ratio of moretane/hopane in my results for Eagle Ford formation is 0.11 (Figure 5.3). Other values of different biomarker ratios for determining thermal maturity are presented in Figure 5.3 and Figure 5.4 with "M" denoted as its application. The inferred vitrinite reflectance value of some biomarker ratios on Figure 5.3 and 5.4 are in parenthesis next to the value.
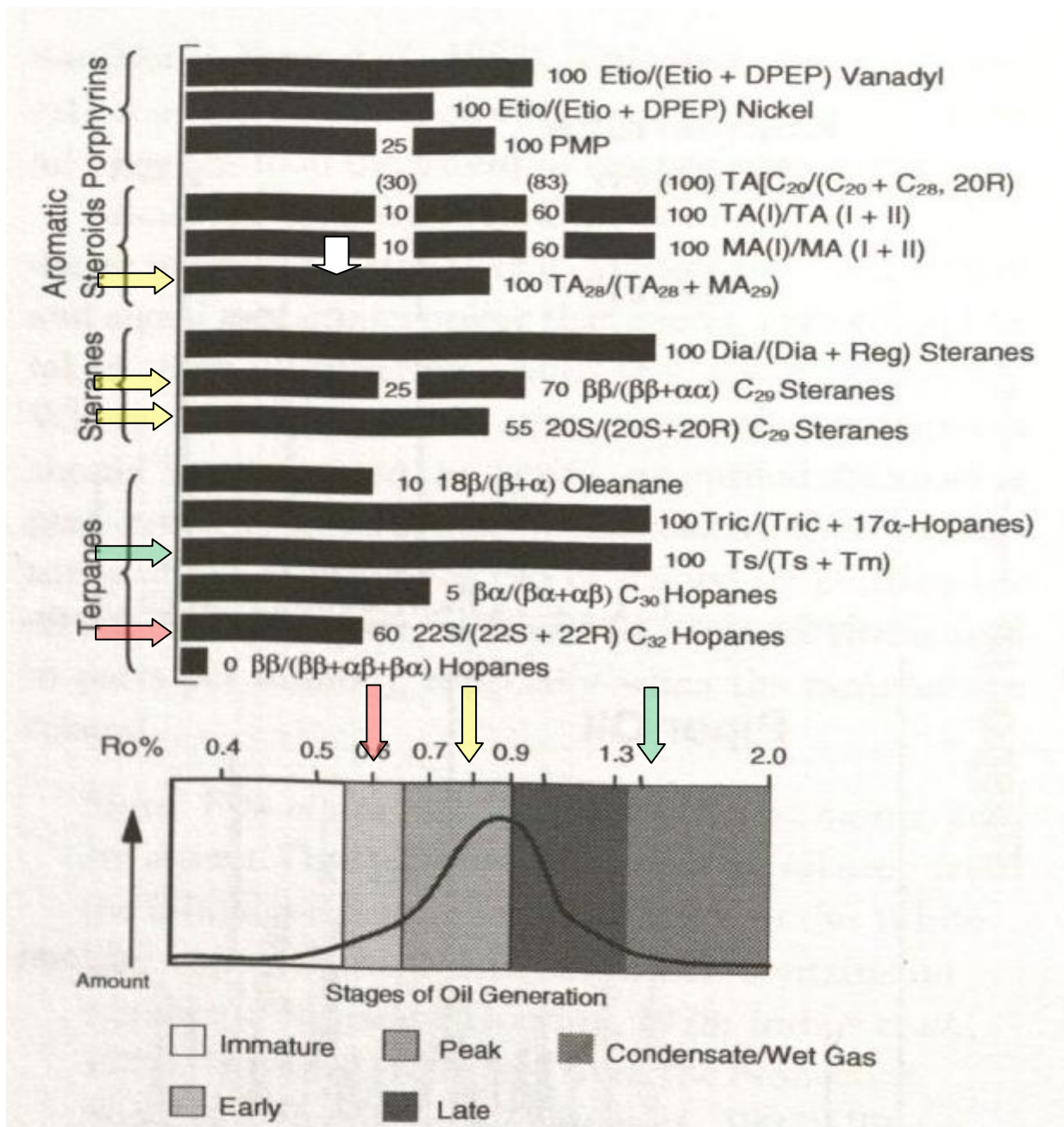
Figure 6.2 Biomarker thermal maturation versus vitrinite reflectance (Peters et al., 2005). The arrows in the figure represent biomarkers in my acquired results and the correlating vitrinite reflectance.

Figure 6.2 shows ranges of biomarker thermal maturity ratios versus vitinite refelctance with a generalized oil-generation curve (after Mackenzie, 1984). The numbers on the bar show the maximum end values, except that 10, 5, and 0 values in the Terpanes section are minimum end values. The solid bars in Figure 6.2 are not linear to the values within; therefore, bars with values within give a more accurate estimation as to where other value lie within the bar. For example, in my acquired results on Figure 5.4 the value for TA28/(TA28+MA29) is 0.59 and a vitrinite reflectance of 0.8 was estimated. Linearly 0.59 will have a vitrinite value that indicates an earlier stage than the peak stage of oil generation on Figure 6.2 (⇩, this symbol is a linear estimate of 0.59 on the bar). The maturity (M) values from my Eagle Ford sample (on Figure 5.3 and 5.4) range from 0.6-1.4% (including a vitrinite value (Ro%) on Figure 5.4 of 0.79). The yellow arrows represent the biomarkers that have a vitrinite reflectance value approximate to 0.79. The red and green arrows represent the biomarkers that are in the early and condensate/wet gas stages of oil generation respectively. The majority of the biomarker values suggest that production may still occur in the reservoir when this oil sample was acquired.

CHAPTER 7

CONCLUSION

Biomarkers are the signature of oils. Prior to biomarker research, the source of an oil sample was speculative. Although there are some limitations in the process of using biomarkers, biomarkers are very important in understanding the source rock properties of oil samples. Some more research can make biomarker parameters more accurate, and can help understand how various variables (like temperature) alter each biomarker.

Section 5.2 contains the Eagle Ford oil sample results I acquired. The following biomarkers from the results show a source rock characteristic of marine shale: pristane/phytane is 1.53; diasteranes/steranes is 2.06 (high); C24 tetracyclic/C26 tricyclics is 0.22 (low); steranes/hopanes ~ 1(high); and oleananes is absent. The absence of oleananes is a characteristic of Cretaceous age. A value of 0.9 derived from the ratio of C28/C29 steranes in Section 5.2 is also a characteristic of Cretaceous age.

As stated in Discussion Section (Chapter 6), a number of the suggested parameters did not match my results in regards to the properties of the Eagle Ford shale formation. Therefore some more research can be done to improve those parameters so that biomarkers suggest similar properties. A few discrepancies are expected in the values because each petroleum system has a unique set of organic matter. Such discrepancies can be seen in biomarker results for my Eagle Ford sample in comparison to other Eagle Ford samples (in Section 5.1 and 5.2).

Also the effect on various biomarkers by variables like temperature need to be studied some more. The thermal maturity biomarkers in my results from the Eagle Ford shale show my sample is in the peak and late stage of generation. This may be due to the different properties of the biomarkers; therefore, the vitrinite reflectance should be altered so that the values infer

50

similar stages of oil generation. Another variable may be thermal stress, and this variable and others should all be studied further to have more accurate parameters.

Finally, my results of the Eagle Ford sample provided tables showing a detailed list of detected compounds. Detailed tables and traces should be made available to the public to further the study of biomarkers.

REFERENCES

Bailey, N.J.L., R. Burwood, and G.E. Harriman. 1990. Application of pyrolyzate carbon isotope and biomarker technology to organofacies definiition and oil correlation problems in North Sea basins. Organic Geochemistry, 16:1157-1172.

Burwood, R. 1999. Angola: source rock control for Lower Congo coastal and Kwanza Basin petroleum system. In: The Oil and Gas Habitat of the South Atlantic (N. Cameron, R.H. Bate and V. Clure, eds.), Geological Society of London, London, 181-194.

Cole, G.A., M.A. Abu-Ali, S.M. Aoudeh, et al. 1994. Organic geochemistry of the Paleozoic petroleum system of Saudi Arabia. Fuel, 8:1425-1442.

Cole, G.A., H.I. Halpern, and S.M. Aoudeh. 1994. The relationships between iron-sulfur-carbon and gamma-ray response, Silurian basal Qusaiba Shale, northern Saudi Arabia. Saudi Aramco Journal of Technology, 95:9-19.

Cole, G.A., A.G. Requejo, D. Ormerod, Z. Yu, and A. Clifford. 2000. Petroleum geochemical assessment of the Lower Congo Basin. In: Petroleum System of South Atlantic Margins (M.R. Mello and B.J. Katz, eds.), American Association of Petroleum Geologists, Tulsa, Ok, 325-339.

Connan, J. 1981. Biological markers in crude oils. In: Petroleum Geology in China (J.F. Mason, ed.), Penn Well, Tulsa, OK, pp. 48-70.

Connan, J., and D. Dessort. 1987. Novel family of hexcyclic hopanoid alkanes (C32-C35) occurring in sediments and oils from anoxic paleoenvironments. Organic Geochemistry, 11:103-113.

Connan, J., J. Bouroullec, D. Dessort and P. Albrecht. 1986. The microbial input in carbonate-anhydrite facies of a sabkha paleoenvironment from Guatemala: A molecular approach. Organic Geochemistry, 10:29-50.

Dahl, J., J.M. Moldowan, and P. Sundararaman. 1993. Relationship of biomarker distribution to depositional en; Phosphoria Formation, Montana, USA. Organic Geochemistry, 20:1001-1017.

Didyk, B.M., B.R.T. Simoneit, S.C. Brassell, and G. Eglinton. 1978. Organic geochemical indicators of paleoenvironmental conditions of sedimentation. Nature, 272:216-222.

Disnar, J., and L.D. Stasiuk. 1996. Organic matter sedimentation in the northeast of the Paris Basin: Consequences in the deposition of the lower Toarcian black shales. Chemical Geology, 131:15-35.

Espitalie, J., F. Marquis, and L. Sage. 1987. Organic geochemistry of the Paris Basin. In: Petroleum Geology of Northwest Europe (J. Brooks and K. Glennie, eds.), Graham and Trotman, London, pp. 71-86.

Fan, P., J.D. King, and G.E. Claypool. 1987. Characteristics of biomarker compounds in Chinese crude oils. In: Petroleum Geochemistry and Exploration in the Afro-Asian Region (R.K. Kumar, P. Dwivedi, V. Banerjie and V. Gupta, eds.), Balkema, Rotterdam, 197-202.

Filiptsov, Y.A., Y.V. Petrishina, L.I. Bogorodskaya, A.A. Kontorovich, and V.A. Krinin. 1999. Evaluation of maturity and oil-and gas-generation properties of organic matter in Riphean and Vendian rocks of the Baykit and Katanga petroleum regions. Geologiya i Geofizika, 40:1362-1374.

Grantham, P.J. and L.L. Wakefield. 1988. Variations in the sterane carbon number distributions of marine source rock derived crude oils through geological time. Organic Geochemistry, 12:61-73.

Halpern, H.I. 1995. Development and application of Light-Hydrocarbon-Based star diagrams. American Association of Petroleum Geologists Bulletin, 79:801-815.

Hatch, J.R., J.R. Jacobson, B.J. Witzke, et al. 1987. Possible Middle Ordovician organic carbon isotope excursion: evidence from Ordovician oils and hydrocarbon source rocks, Mid-Continent, and East-Central United States. American Association of Petroleum Geologists Bulletin, 71:1342-1354.

Higley, D.K. 2002. The Talara Basin province of northwestern Peru: Cretaceous-Tertiary total petroleum system. Presented at the Annual Meeting of the American Association of Petroleum Geologists, March 10-13, 2002, Houston, TX.

Holba, A.G., L.I.P. Dzou, and W.D. Masterson. 1998. Application of 24-norcholestanes for constraining source age of petroleum. Organic Geochemistry, 29:1269-1283.

Holba, A.G., L. Ellis, L.I.P. Dzou, et al. 2001. Extended tricyclic terpanes as age discriminators between Triassic, Early Jurassic and Middle-Late Jurassic oils. Presented at the 20th International Meeting on Organic Geochemistry, 10-14 September, 2001, Nancy France.

Hughes, W.B. 1984. Use of thiophenic organosulfur compounds in characterizing crude oils derieved from carbonate versus siliciclastic sources. In: Petroleum Geochemistry and Source Rock Potential of Carbonate Rocks (J.G. Palacas, ed.), American Association of Petroleum Geologists, Tulsa, OK, 181-196.

Jarvie, D.M., R.J., Hill, T.E.Ruble, and R.M. Pollastro, R.M. 2007. Unconventional shale-gas system: The Mississippian Barnet Shale of north-central Texas as one model of thermogenic shale-gas assessment. American Association of Petroleum Geology Bulletin, 91(4):475-499.

Jewell, P.W., 1995. Geological consequences of globe-encircling equatorial currents. Geology, 23:117-120.

Jones, P.J. and T.E. Stump. 1999. Depositional and tectonic setting of the Lower Silurian hydrocarbon source rock facies, central Saudi Arabia. American Association of Petroleum Geologists Bulletin, 83:314-332.

Katz, B.J. 1995. The Schistes Carton – the Lower Toarcian of the Paris Basin. In: Petroleum Source Rocks, Casebooks in Earth Science (B.J. Katz, ed.), Springer-Verlag, Berlin, pp. 61-79.

Kupecz, J.A. 1995. Depositional setting, sequence stratigraphy, diagensis, and reservoir potential of a mixed-lithology, upwelling deposit: Upper Triassic Shublik Formation, Prudhoe Bay, Alaska. American Association of Petroleum Geologists Bulletin, 79:1301-1319.

Lambert, M.W. 1993. Internal stratigraphy and organic facies of the Devonian-Mississipian Chattanooga (Woodford) Shale in Oklahoma and Kansas. In: Source Rocks in a Sequence Stratigraphy Framework, (B.J. Katz and L.M. Pratt, eds.), American Association of Petroleum Geologists, Tulsa, OK, 163-176.

Lambert, M.W., P.J. Burkett, W.A. Chiou, R.H. Bennett, and D.M. Lavoie. 1994. Kerogen networks and hydrocarbon generation in the Chattanooga (Woodford) Shake of Oklahoma and Kansas. Presented at the Annual Meeting of American Association of Petroleum Geologists, June 12-15, 1994, Denver, CO.

Lewan, M.D. 1983. Effects of thermal maturation of stable organic carbon isotopes as determined by hydrous pyrolysis of Woodford Shale. Geochimica et Cosmochimica Acta, 47:1471-1479.

Mackenzie, A.S. 1984. Application of biological markers in petroleum geochemistry. In: Advances in Petroleum Geochemistry Vol.1 (J. Brooks and D.H. Welte, eds.), Academic Press, London, pp. 115-214.

Mackenzie, A.S., C. Beaumont, and D.P. McKenzie. 1984. Estimation of the kinetics of geochemical reactions with geophysical models of sedimentary basins and applications. Organic Geochemistry, 6:875-84.

Maitland, J.J. 2000. Organic Chemistry. 2nd edition, W. W. Norton & Company, Inc., 500 fifth Avenue, New York, NY 10110.

Mango, F.D. 1994. The origin of Light-Hydrocarbons in petroleum - Ring preference in the closure of carbocyclic rings. Geochimica et Cosmochimica Acta, 58:895-901.

Marshall, J.E.A., D.A. Rogers, and M.J. Whiley. 1996. Devonian marine incursions into the Orcadian Basin, Scotland. Journal of the Geological Society of London, 153:451-466.

Marzi, R., B.E. Torkelson, and R.K. Olson. 1993. A revised carbon preference index. Organic Geochemistry, 20:1301-1306.

Maughan, E.K. 1993. Phosphoria Formation (Permian) and its resource significance in the Western Interior, USA. Presented at the CSPG Pangeo: Global Environment and Resources Conference, Calgary, August 15-19, 1993.

McKirdy, D.M., A.K. Aldridge and P.J.M. Ypma. 1983. A geochemical comparison of some crude oils from Pre-Ordovician carbonate rocks. In: Advances in Organic Geochemistry 1981 (M. Bjoroy, C. Albrecht, C. Cornford et al., eds.), John Wiley & Sons, New York, pp. 99-107.

Michels, R., P. Landais, B.E. Torkelson, and R.P. Philp. 1995. Effects of effluents and water pressure on oil generation during confined pyrolysis and high pressure hydrous pyrolysis. Geochimica et Cosmochimica Acta, 59:1589-1604.

Moldowan, J.M. 2000. Trails of life. Chemistry in Britain, 36:34-37.

Moldowan, J.M., J. Dahl, S.R. Jacobson, B.J. Huizinga, F.J. Fago, R. Shetty, D.S. Watt, and K.E. Peters. 1996. Chemostratigraphic reconstruction of biofacies: Molecular evidence linking cyst-forming dinoflagellates with pre-Triassic ancestors. Geology, 24:159-162.

Moldowan, J.M., B.J. Huizinga, J.E. Dahl, F.J. Fago, D.W. Taylor, and L.J. Hickey. 1994. The molecular fossil record of oleanane and its relationship to angiosperms. Science, 265:768-771.

Moldowan, J.M., and S.R. Jacobson. 2000. Chemical signals for early evolution of major taxa: biosignatures of taxon-specific biomarkers. International Geology Review, 42:805-812.

Moldowan, J.M., S.R. Jacobson, J. Dahl, A. Al-Hajji, B.J. Huizinga, and F.J. Fago. 2001. Molecular fossils demonstrate Precambrian origin of dinoflagellates. In: Ecology of the Cambrian Radiation (A. Zhuravlev and R. Ridings, eds), Columbia University Press, New York, pp. 474-493.

Moldowan, J.M., W.K. Seifert, and E.J. Gallegos. 1985. Relationship between petroleum composition and depositional environment of petroleum source rocks: American Association of Petroleum Geologists Bulletin, 69:1255-1268.

Montgomery, S. 1990. Tight gas formation: an ongoing effort by the U.S. Department of Energy. Petroleum Frontiers, 7:26-35.

Palacas, J.G. 1984. Carbonate rocks as sources of petroleum geological and chemical characteristics and oil-source correlations. In: Proceedings of the Eleventh World Petroleum Congress 1983, Volume 2, John Wiley & Sons, Chictester, UK, pp. 31-43.

Pancost R.D., K.H. Freeman, and M.E. Patzkowsky. 1999. Organic-matter source variation and the expression of a late Middle Ordovician carbon isotope excursion. Geology, 27:1015-1018.

Parrish, T.J. 1982. Upwelling and petroleum source beds, with reference to Paleozoic. American Association of Petroleum Geologists Bulletin, 66:750-774.

Peters, K.E., M.J. Clutson, and G. Robertson. 1999. Mixed marine and lacustrine input to an oil-cemented sandstone breccia from Brora, Scotland. Organic Geochemistry, 30:237-248.

Peters, K.E., J.M. Moldowan, A.R. Driscole, and G.J. Demaison. 1989. Origin of Beatrice oil by cosourcing from Devonian and Middle Jurassic source rock, Inner Morary Firth, UK. American Association of Petroleum Geologists Bulletin, 73:454-471.

Peters, K.E. and J.M. Moldowan. 1993. The Biomarker Guide: Interpreting Molecular Fossils in Petroleum and Ancient Sediments. Prentice-Hall, Englewood Cliffs, NJ.

Peters, K.E., C.C.Walters, and J.M. Moldowan. 2005. The Biomarker Guide. 2nd volume, Cambridge Press, New York, NY, pp. 475-963.

Philp, R.P., J. Li, and C.A. Lewis. 1989. An organic geochemical investigation of crude oils from Shanganning, Jianghan, Chaidamu and Zhungeer basins, People's Republic of China. Organic Geochemistry, 14:447-460.

Pollastro, R.M. 1999. Ghaba Salt Basin Province and Fahud Salt Basin Province, Oman-geological overview and total petroleum systems. In: U.S. Geological Survey Bulletin, 2167:41.

Railroad Commission of Texas. 2012. Eagle Ford Information. Retrieved on April 3, 2012 from http://www.rrc.state.tx.us/eagleford/index.php.

Richnow, H.H., A. Jenisch and W. Michaelis. 1992. Structural investigations of sulphur-rich macromolecular oil fractions and a kerogen by sequential chemical degradation. Organic Geochemistry, 19:351-370.

Riolo, J., G. Hussler, P. Albrecht, and J. Connan. 1986. Distribution of aromatic steroids in geological samples: their evaluation as geochemical parameters. Organic Geochemistry, 10:981-90.

Robison, C.R. 1997. Hydrocarbon source rock variability within the Austin Chalk and Eagle Ford Shale (Upper Cretaceous), East Texas, U.S.A. International Journal of Coal Geology, 34:287-305.

Schoellkopf, N.B. and B. Patterson. 2000. Petroleum system of offshore Cabinda, Angola. In: Petroleum Systems of South Atlantic Margins (M.R. Mello amd B.J. Katz, eds.), American Association of Petroleum Geologists, Tulsa, OK, 361-176.

Seifert, W.K. and J.M. Moldowan. 1980. The effect of thermal stress on source-rock quality as measured by hopane stereochemistry. Physics and Chemistry of the Earth, 12:229-237

Seifert, W.K. and J.M. Moldowan. 1986. Use of biological markers in petroleum exploration. In Methods in Geochemistry and Geophysics Vol. 24 (R. B. Johns, ed.), Elsevier, Amsterdam, pp. 261-290.

Ten Haven, H.L., J.W. de Leeuw, J. Rullkotter, and J.S. Sinninghe Damste. 1987. Restricted utility of the pristane/phytane ratio as a paleoenvironmental indicator. Nature, 330:641-643.

Ten Haven, H.L., J.W. de Leeuw, J.S. Sinninghe Damste, et al. 1988. Application of biological markers in the recognition of palaeohypersaline environments. In: Lacustrine Petroleum Source Rocks (A.J. Fleet, K. Kelts and M.R. Talbot, eds.), Blackwell, London, pp. 123-130.

Terken, J.M.J., N.L. Frewin, and S.L. Indrelid. 2001. Petroleum system of Oman: charge timing and risks. American Association of Petroleum Geologists Bulletin, 85:1817-1845.

Thompson, K.F.M. 1983. Classification and thermal history of petroleumbased on light hydrocarbons. Geochimica et Cosmochimica Acta, 47:303-316.

Tissot, B.P. and D.H. Welte. 1984. Petroleum Formation and Occurrence. Springer-Verlag, New York.

Tissot, B., J. Espitalie, G. Deroo, C. Tempere, and D. Jonathan. 1984. Origin and migration of hydrocarbons in the eastern Sahara (Algeria), In: Petroleum Geochemistry and Basin Evaluation, (G. Demaison and R.J. Murris, eds.), American Association of Petroleum Geologists, pp. 315-324

Tyson, R.V. 1995. Sedimentary Organic Matter: Organic Facies and Palynofacies. Chapman and Hall, New York.

Wang, H.D. and R.P. Philip. 1997. Geochemical study of potential source rocks and crude oils in the Anadarko Basin, Oklahoma. America Association of Petroleum Geologists Bulletin, 81:249-275.

Winters, J.C., and J.A. Williams. 1969. Microbiological alteration of crude oil in the reservoir. American Chemical Society, Division of Petroleum Chemistry, New York Meeting Preprints, v. 14(4), p. E22-E31.

World Oil. 2012. Retrieved on June 6, 2012 from http://www.worldoil.com/Oil-NGL-and-condensate-opportunities-lift-Eagle-Ford-Shale-activity.html.

BIOGRAPHICAL INFORMATION

Ugochukwu Ononogbu began a Bachelors Degree at the University of Texas at Arlington in the spring of 2007, which he completed in the spring of 2010 with a Bachelors Degree in Geology and a minor in Chemistry. He began pursuing a Masters Degree at the University of Texas at Arlington and is projected to graduate in the fall of 2012 with a Masters Degree in Geology. He has research interests in oil exploration fields ranging from structural and sedimentary properties of reservoirs to the geochemistry of oil and gas. He has worked on projects that encompass structural geology, sedimentary geology, paleontology, metamorphism, petrology etc. Furthermore, he has worked on projects that directly prepare students for professional work: seismic, mapping, and geo-steering software based projects. Ugochukwu Ononogbu hopes to someday follow in his father's footsteps by working for an energy producing company.